ISSN 2096-7071 (Print)
ISSN 2097-3101 (Online)
CN 10-1629/R1

CHINA CDC WEEKLY

Vol. 8 No. 18 May 1, 2026

中国疾病预防控制中心周报(英文)

ISSN 2096-7071

China CDC Weekly

Editorial Board

Editorial Office

Cover Image: adapted from National Disease Control and Prevention Administration, https://www.ndcpa.gov.cn/jbkzzx-/c100008/common/content/content_2039981305493884928.html.

Commentary

World Malaria Day 2026: Driven to End Malaria

Xiaonong Zhou[1,2,#]; Junhu Chen[1,2]; Zhigui Xia[1]; Shizhu Li[1]

On April 25, 2026, the world observes World Malaria Day under the theme "Driven to End Malaria: Now We Can. Now We Must." Established by the World Health Organization (WHO) member states in 2007, this annual event rallies global consensus in the fight against malaria, one of the most devastating mosquito-borne infectious diseases (*1*). Between 2000 and 2024, malaria control interventions averted an estimated 2.3 billion cases and 14 million deaths worldwide. Effective tools — including insecticide-treated nets (ITNs), seasonal malaria chemoprevention (SMC), and malaria vaccines — have driven these gains (*2*). Already, 25 countries are deploying malaria vaccines to protect 10 million children annually, next-generation mosquito nets account for 84% of all newly distributed nets, and approximately 37 countries reported fewer than 1,000 cases in 2024. Momentum continues: Georgia, Suriname, and Timor-Leste achieved malaria-free certification in 2025, bringing the global total to 47 countries and one territory. Yet the resurgence of malaria in Cabo Verde following certification underscores the fragility of these achievements (*2*). For China, which received WHO malaria-free certification in 2021 (*3*), the current priority is consolidating elimination gains and preventing the re-establishment of local transmission through imported cases. Drawing on the evolution of World Malaria Day and the 2026 theme, this article analyzes technical bottlenecks in global malaria control, examines the impact of the persisting global epidemic on China's elimination achievements, and proposes a dual-track strategy combining strengthened domestic vigilance with active participation in global governance.

Current Global Malaria Status and Major Technical Challenges

Despite millennia of efforts to combat malaria, the disease remains a formidable threat to global public health. The World Malaria Report 2025 reveals that the global burden continues to grow: an estimated 282 million cases and 610,000 deaths occurred in 2024, representing increases of 3% (approximately 9 million cases) and 2% (approximately 12,000 deaths) compared with 2023 (*2*). After declining by 25.6% between 2000 and 2015, case incidence rose by 8.5% from 2015 to 2024, while the mortality rate held steady at 13.8 per 100,000 population at risk. Progress toward the Global Technical Strategy (GTS) 2025 targets has fallen significantly off track — the 2024 incidence stands at 3.5 times the target, and the mortality rate at three times the target (*2*). Sub-Saharan Africa bears the overwhelming burden, accounting for approximately 94% of all cases (265 million) and 95% of all deaths (579,000) in 2024. Five countries alone — Nigeria, the Democratic Republic of the Congo, Uganda, Ethiopia, and Mozambique — contributed nearly half of all global cases, underscoring the extreme geographic concentration of the disease (*2*).

Three interconnected categories of factors drive this rising burden. First, biological challenges have intensified: antimalarial drug resistance continues to spread (e.g., artemisinin partial resistance confirmed in Eritrea, Rwanda, Uganda, and the United Republic of Tanzania) (*2*,*4*), *pfhrp2/3* gene deletions increasingly compromise diagnostic accuracy (*5*–*6*), and insecticide resistance among vector mosquitoes has become widespread (*7*–*8*). Second, systemic and operational weaknesses persist, including suboptimal intervention delivery, limited access to quality healthcare, surveillance gaps, and frequent stock-outs of essential commodities (*2*,*9*). Third, external disruptions compound these challenges — notably armed conflict and insecurity (e.g., in Ethiopia, Sudan, and Yemen), climate-related events (e.g., in Madagascar), and significant reductions in international development assistance (*2*).

Underlying this heavy disease burden are critical technological bottlenecks and external challenges. First, biological resistance poses an escalating threat to future malaria epidemiology. *Plasmodium falciparum* resistance to artemisinin-based combination therapies (ACTs) — the cornerstone of current treatment — has emerged in parts of the Greater Mekong Subregion and several African regions, directly jeopardizing

frontline therapeutic strategies (*10*–*12*). Simultaneously, *Anopheles* spp. mosquitoes are rapidly developing resistance to mainstream insecticides such as pyrethroids, substantially eroding the protective efficacy of insecticide-treated bed nets and other conventional vector control tools (*7*,*13*). Second, a significant gap persists in the development and deployment of innovative tools. Although World Malaria Day themes in 2022 and 2023 highlighted "innovation" and "investment, innovation, implementation," respectively, vaccine development remains insufficient. Beyond the recent pilot rollout of RTS, S and R21 vaccines in Africa, the field still lacks highly effective, affordable, and broadly applicable vaccines suited to diverse epidemiological settings (*14*–*15*). Furthermore, climate change is altering temperature and precipitation patterns, reshaping mosquito vector habitats and exposing previously non-endemic areas to new transmission risks, thereby compounding the technical challenges of global control (*16*). Arguably the most significant factor, however, is the weakening of intervention capacity during the post-pandemic period, driven by the worldwide economic downturn.

Impact and Challenges of Rising Global Epidemic on China's Consolidation of Elimination Achievements

China officially received WHO certification for malaria-free status in 2021, marking a milestone in the nation's public health history (*3*). However, the 2026 World Malaria Day theme — "Driven to End Malaria: Now We Can. Now We Must" — underscores that the global epidemic has not yet reached a turning point and that concerted international action remains essential to achieve worldwide elimination. This landscape of high external risk and low internal transmission poses severe challenges to China's efforts to consolidate its elimination achievements.

First, imported cases continue to exert persistent pressure, and the challenge of preventing re-transmission remains acute, particularly in border areas such as Yunnan Province (*17*). China maintains extensive economic, trade, and personnel ties with highly endemic regions in Southeast Asia and Africa. Between 2017 and 2024, China reported 16,571 imported cases, with the annual number rebounding steadily since 2021 to reach 3,155 in 2024 (*18*) — predominantly from high-burden countries including Nigeria, the Democratic Republic of the Congo, and Myanmar. In Myanmar's border areas adjacent to Yunnan, malaria cases surged from just 2,583 in 2019 to 34,171 in 2024, while imported cases in Yunnan rose to 564 in the same year (*19*). Frequent cross-border movement and shared ecological landscapes sustain vector mosquito populations, including *Anopheles minimus*, along these borders. Without prompt detection and containment of imported cases, secondary local transmission can readily occur, creating a high risk of resurgence (*20*). The WHO's data confirming a global rebound in malaria incidence further intensifies the pressure on China's port quarantine and disease control systems (*2*).

Second, the risk of post-elimination complacency and eroding technical capacity looms large. As indigenous cases disappear, malaria prevention and control efforts become increasingly invisible and susceptible to neglect. In primary healthcare facilities, younger clinicians lack firsthand diagnostic experience with malaria's hallmark symptoms — periodic chills and high fever — elevating the risks of misdiagnosis and delayed treatment (*21*). The 2017 World Malaria Day theme, "Malaria Elimination: Let's Bridge the Gap," carries renewed significance for China today: if post-elimination surveillance systems lose their sensitivity and gaps emerge in the specialized workforce, the country's malaria-free achievement will become increasingly vulnerable (*22*).

China's Path to Consolidating Elimination Achievements and Deepening Global Cooperation

Confronting the current stalemate in global malaria control, China should seize the momentum of World Malaria Day 2026 and embrace the spirit of "Driven to End Malaria: Now We Can. Now We Must" by pursuing a dual-track strategy: strengthening domestic defenses against importation while actively contributing to global efforts. In doing so, China can share its expertise toward building a global community of shared health.

Strengthening Internal Defenses: Precise Measures to Prevent Re-Transmission of Imported Malaria

The core of domestic prevention lies in maintaining a robust surveillance and response system alongside strong clinical treatment capabilities.

First, China must reinforce implementation of the

"1-3-7" surveillance and response approach (*23*). This pioneering framework — case reporting within 1 day, investigation within 3 days, and focus response within 7 days — has been formally incorporated into WHO technical guidelines (*24*). With thousands of imported cases arriving annually, rigorous enforcement is essential, particularly through precise management of border areas and migrant worker populations, to ensure timely, standardized handling of every focus and decisively interrupt potential transmission chains.

Second, primary healthcare capacity and public awareness must be strengthened. Because most imported cases involve *Plasmodium falciparum* — which carries a high risk of progressing to severe disease — targeted training for medical staff in key areas should enhance microscopy skills and ensure standardized use of antimalarial drugs (*25*). Alongside World Malaria Day campaigns, efforts should promote self-protection awareness among outbound workers and border residents. Concurrently, county-level risk maps for malaria transmission re-establishment should be updated annually.

Finally, vector surveillance and environmental management must be strengthened. Ongoing monitoring of mosquito density and insecticide resistance, combined with elimination of breeding sites through patriotic health campaigns and a One Health approach, will reduce transmission risk at its source (*26*). Expanding the establishment of mosquito risk-free communities will further help interrupt potential malaria transmission.

Deepening Global Participation: Implementing Partnerships to Promote the Achievement of SDGs

A central goal of World Malaria Day 2026 is to advance the United Nations Sustainable Development Goals (SDGs), particularly SDG 17 (Partnerships) (*27*). As a responsible major country, China should actively contribute to global malaria control, thereby reducing the worldwide burden and indirectly alleviating import pressure at home. On one hand, China can share proven solutions and technical expertise. The "1-3-7" surveillance and response approach, antimalarial drug research and development — spanning discovery, clinical trials, regulatory approval, and public health deployment — and vector control technologies all offer valuable models for African and Southeast Asian countries. Through South-South cooperation mechanisms, China should support health system capacity-building in high-burden nations by providing technical training, material assistance, and on-site guidance (*28*). On the other hand, China must strengthen international cooperation in research and innovation. Responding to the calls for innovation issued on World Malaria Day in 2022 and 2023, Chinese research institutions and enterprises should deepen collaboration with the WHO and relevant international organizations, focusing on critical global challenges such as drug resistance, vaccine development, and novel vector control tools. Chinese scientists, in particular, can play a distinctive role in monitoring and addressing artemisinin resistance, contributing vital scientific and technological support to global malaria control and elimination efforts.

CONCLUSION

On World Malaria Day 2026, the World Health Organization and its partners launch the campaign "Driven to End Malaria: Now We Can. Now We Must," a rallying cry for global public health and a resolute response to the complex realities of worldwide malaria transmission. The staggering burden of hundreds of millions of cases each year reminds us that malaria remains an ever-present threat. For China, elimination is not the finish line but the start of a new chapter. The nation must remain vigilant in preventing re-transmission from the thousands of imported cases arriving annually, while also looking outward — actively advancing SDG 3's goal of "good health and well-being" by sharing experience, providing technical assistance, and strengthening scientific cooperation with high-burden countries. Only by uniting globally, closing persistent gaps, and driving innovation can we transform the vision of a malaria-free world into reality.

Conflicts of interest: No conflicts of interest.

doi: 10.46234/ccdcw2026.087

[#] Corresponding author: Xiaonong Zhou, zhouxn1@chinacdc.cn.

[1] National Key Laboratory of Intelligent Tracking and Forecasting for Infectious Diseases, National Institute of Parasitic Diseases, Chinese Center for Disease Control and Prevention (Chinese Center for Tropical Diseases Research), NHC Key Laboratory for Parasitology and Vector Biology, WHO Collaborating Centre for Tropical Diseases, National Centre for International Research on Tropical Diseases, Shanghai, China; [2] Hainan Tropical Diseases Research Center (Hainan Sub-Center, Chinese Center for Tropical Diseases Research), Haikou City, Hainan Province, China.

Submitted: March 25, 2026
Accepted: April 24, 2026
Issued: May 01, 2026

REFERENCES

1. World Health Organization. WHA60.18: malaria including proposal for establishment of World Malaria Day. Geneva: World Health Organization; 2007. https://www.afro.who.int/publications/wha6018-malaria-including-proposal-establishment-world-malaria-day.
2. World Health Organization. World malaria report 2025. Geneva: World Health Organization; 2025. https://www.who.int/publications/i/item/9789240117822.
3. World Health Organization. World malaria report 2021. Geneva: World Health Organization; 2021. https://www.who.int/teams/global-malaria-programme/reports/world-malaria-report-2021.
4. Rosenthal PJ, Asua V, Bailey JA, Conrad MD, Ishengoma DS, Kamya MR, et al. The emergence of artemisinin partial resistance in Africa: how do we respond?. Lancet Infect Dis 2024;24(9):e591 – 600. https://doi.org/10.1016/S1473-3099(24)00141-5.
5. Molina-de la Fuente I, Pastor A, Herrador Z, Benito A, Berzosa P. Impact of *Plasmodium falciparum pfhrp2* and *pfhrp3* gene deletions on malaria control worldwide: a systematic review and meta-analysis. Malar J 2021;20(1):276. https://doi.org/10.1186/s12936-021-03812-0.
6. Watson OJ, Tran TNA, Zupko RJ, Symons T, Thomson R, Visser T, et al. Global risk of selection and spread of *Plasmodium falciparum* histidine-rich protein 2 and 3 gene deletions. Nat Med 2025;31(10):3372 – 9. https://doi.org/10.1038/s41591-025-03974-3.
7. Pelloquin B, Agossa F, Acford-Palmer H, Clark T, Ogoma SB, Williams M, et al. Novel insecticide resistance mutations associated with variable PBO synergy in *Anopheles gambiae* s. l. from the Democratic Republic of Congo. Sci Rep 2025;15(1):27618. https://doi.org/10.1038/s41598-025-09016-9.
8. Ondeto BM, Nyundo C, Kamau L, Muriu SM, Mwangangi JM, Njagi K, et al. Current status of insecticide resistance among malaria vectors in Kenya. Parasit Vectors 2017;10(1):429. https://doi.org/10.1186/s13071-017-2361-8.
9. Huang SK, Khan J, Lokang F, Ayuiel AR, Baker K, Julla A, et al. Development of a new wealth index for South Sudan: association between household wealth and malaria prevention practices in the context of seasonal malaria chemoprevention in northern Bahr el Ghazal, South Sudan. Infect Dis Poverty 2025;14(1):57. https://doi.org/10.1186/s40249-025-01327-3.
10. Uwimana A, Umulisa N, Venkatesan M, Svigel SS, Zhou ZY, Munyaneza T, et al. Association of *Plasmodium falciparum kelch13* R561H genotypes with delayed parasite clearance in Rwanda: an open-label, single-arm, multicentre, therapeutic efficacy study. Lancet Infect Dis 2021;21(8):1120 – 8. https://doi.org/10.1016/S1473-3099(21)00142-0.
11. Dhorda M, Amaratunga C, Dondorp AM. Artemisinin and multidrug-resistant *Plasmodium falciparum* – a threat for malaria control and elimination. Curr Opin Infect Dis 2021;34(5):432 – 9. https://doi.org/10.1097/QCO.0000000000000766.
12. Ndwiga L, Kimenyi KM, Wamae K, Osoti V, Akinyi M, Omedo I, et al. A review of the frequencies of *Plasmodium falciparum* Kelch 13 artemisinin resistance mutations in Africa. Int J Parasitol Drugs Drug Resist 2021;16:155 – 61. https://doi.org/10.1016/j.ijpddr.2021.06.001.
13. Julius N, Diane BI. Investigating the resurgence of malaria in Rwanda: factors contributing to rising cases amidst near-eradication success and strategies for sustained control. Ann Med Surg 2025;87(11):7363 – 8. https://doi.org/10.1097/MS9.0000000000003912.
14. Macià D, Pons-Salort M, Moncunill G, Dobaño C. The effect of disease transmission on time-aggregated treatment efficacy estimates: a critical analysis of factors influencing the RTS,S and R21 malaria vaccine phase 3 trials. Lancet Infect Dis 2025;25(9):e516 – 26. https://doi.org/10.1016/S1473-3099(25)00090-8.
15. Datoo MS, Natama MH, Somé A, Traoré O, Rouamba T, Bellamy D, et al. Efficacy of a low-dose candidate malaria vaccine, R21 in adjuvant Matrix-M, with seasonal administration to children in Burkina Faso: a randomised controlled trial. Lancet 2021;397(10287):1809 – 18. https://doi.org/10.1016/S0140-6736(21)00943-0.
16. Mordecai EA, Ryan SJ, Caldwell JM, Shah MM, LaBeaud AD. Climate change could shift disease burden from malaria to arboviruses in Africa. Lancet Planet Health 2020;4(9):e416 – 23. https://doi.org/10.1016/S2542-5196(20)30178-9.
17. Zheng DS, Tian P, Yan GY, Lin ZR, Zhou HN, Liu XB, et al. Stratified vector control and proactive cross border collaboration for sustaining malaria elimination in Yunnan, China. BMJ 2025;389:e082300. https://doi.org/10.1136/bmj-2024-082300.
18. Zhang L, Xia ZG, Li SZ. Epidemiological characteristics of malaria in China, 2024. Chin J Parasitol Parasit Dis 2025;43(2):162-6. http://dx.doi.org/10.12140/j.issn.1000-7423.2025.02.002. (In Chinese).
19. Lin ZR, Shao ZT, Xia ZG. Achievements, experience and challenges in preventing importation and re-transmission of malaria in the China-Myanmar border area of Yunnan Province. China Trop Med 2026;26(1):41 – 4. https://doi.org/10.13604/j.cnki.46-1064/r.2025-1460.
20. Liu BW, Zhang T, Wang DQ, Xia S, Li WD, Zhang XX, et al. Profile and determinants for complications of imported malaria in 5 Chinese provinces from 2014 to 2021: retrospective analysis. JMIR Public Health Surveill 2024;10:e52089. https://doi.org/10.2196/52089.
21. Atobatele S, Mpimbaza A, Ngufor C, Yavo W, Konate-Toure A, Ahogni I, et al. Characteristics of healthcare workers and health facilities associated with inaccurate recording of malaria rapid diagnostic test results: a multi-country study. Malar J 2025;25(1):4. https://doi.org/10.1186/s12936-025-05674-2.
22. World Health Organization. World Malaria Day 2017-malaria prevention: let's close the gap. Geneva: World Health Organization; 2017. https://www.who.int/news-room/events/detail/2017/04/25/default-calendar/world-malaria-day-2017.
23. Zhou SS, Zhang SS, Zhang L, Rietveld AEC, Ramsay AR, Zachariah R, et al. China's 1-3-7 surveillance and response strategy for malaria elimination: is case reporting, investigation and foci response happening according to plan?. Infect Dis Poverty 2015;4(1):55. https://doi.org/10.1186/s40249-015-0089-2.
24. World Health Organization. A framework for malaria elimination. Geneva: World Health Organization; 2017. https://www.who.int/publications/i/item/9789241511988.
25. Rotejanaprasert C, Malaphone V, Mayxay M, Chindavongsa K, Banouvong V, Khamlome B, et al. Malaria epidemiology, surveillance and response for elimination in Lao PDR. Infect Dis Poverty 2024;13(1):35. https://doi.org/10.1186/s40249-024-01202-7.
26. Zhang XX, Guo XK, Zhou XN. One Health: a key element in the WHO Pandemic Agreement. Lancet 2025;405(10496):2197 – 8. https://doi.org/10.1016/S0140-6736(25)01118-3.
27. Nikolaou CK. Editorial: nutrition and sustainable development goal 17: partnerships for the goals. Front Nutr 2024;11:1480618. https://doi.org/10.3389/fnut.2024.1480618.
28. Li HM, Arthur Djibougou D, Lu SN, Lv S, Zongo D, Wang DQ, et al. Strengthening capacity-building in malaria and schistosomiasis control under China-Africa cooperation: assessing a case study of Burkina Faso. Sci One Health 2022;1:100009. https://doi.org/10.1016/j.soh.2023.100009.

Vital Surveillances

Epidemic Status of Soil-Transmitted Helminthiasis — China, 2023–2024

Huihui Zhu[1]; Jilei Huang[1]; Changhai Zhou[1]; Tingjun Zhu[1]; Luyuan Zhao[1]; Shizhu Li[1,2,#]; Menbao Qian[1,#]

Summary

What is already known about this topic?

Established in 2016, China's national surveillance system for soil-transmitted helminthiasis provides annual data that are essential for its control. Surveillance data from 2016 to 2022 indicated a steady decline in the overall infection rate, from 2.46% in 2016 to 0.64% in 2022.

What is added by this report?

In 2023 and 2024, the infection rates of soil-transmitted helminth (STH) were 0.53% and 0.47%, respectively, according to national surveillance. The overall infection rate has declined since 2016.

What are the implications for public health practice?

Soil-transmitted helminthiasis exhibits a low prevalence nationwide, yet displays significant geographical and demographic heterogeneity, as well as ongoing transmission risks. Tailored strategies must be implemented to strengthen national control efforts, advance transmission control and prevent interruptions.

ABSTRACT

Introduction: This study reports on 2023–2024 national surveillance data from China's soil-transmitted helminthiasis surveillance network, which covers over 400 counties across 31 provincial-level divisions (PLADs) and the Xinjiang Production and Construction Corps (XPCC). These findings aim to guide future control strategies.

Methods: In 2023 and 2024, each PLAD will select 10%–15% of its jurisdictions as annual surveillance counties, resulting in 437 and 459 counties being chosen, respectively. Using geographically stratified cluster random sampling, 1,000 participants were enrolled in each county. Stool samples from all participants and soil samples from five households in each village were collected and examined. Infection rates and intensities were calculated and compared using the Chi-square test.

Results: In 2023 and 2024, the infection rates of soil-transmitted helminth (STH) were 0.53% (2,381/449,220) and 0.47% (2,233/476,756) , respectively, with significant differences. High STH prevalence was concentrated in Sichuan, Yunnan, and Chongqing in both years, with obvious infection heterogeneity according to sex and age. Hookworm infection was the dominant type, followed by *Ascaris lumbricoides* and *Trichuris trichiura*. Environmental soil monitoring confirmed the presence of Ascaris eggs and hookworm larvae.

Conclusion: Despite the low overall prevalence, soil-transmitted helminthiasis in China remains geographically and demographically heterogeneous. Targeted strategies are required to strengthen control measures and work toward control and eventual interruptions.

Soil-transmitted helminths (STH), primarily hookworms, *Ascaris lumbricoides* and *Trichuris trichiura* (*1*), pose a major health threat in China. Heavy infections cause intestinal damage, leading to malnutrition, stunting, anemia, impaired immune function in children, and adverse pregnancy outcomes (*2–3*). Despite historical declines in prevalence due to control programs and improved living standards, STHs remain widely distributed (*4–6*). A 2015 national survey on key parasitic diseases reported an overall STH infection rate of 4.49% in China, corresponding to an estimated 29.12 million infected individuals (*6*).

In 2016, China integrated STH surveillance into a Central Government-funded Project for the Control of Malaria and Other Key Parasitic Diseases, establishing a nationwide surveillance system (*7*). From 2016 to 2022, the national STH surveillance program gradually expanded to over 400 monitoring counties across all 31 provincial-level divisions (PLADs) and the Xinjiang Production and Construction Corps (XPCC).

Epidemiological patterns of STH infections have evolved (*7–13*). Using 2023–2024 national STH surveillance data, this study analyzed infection status in China to provide evidence for future control strategies.

METHODS

Study Population and Sampling

National surveillance across all 31 PLADs and the XPCC in 2023–2024 will employ a stratified cluster random sampling design. Annually, each PLAD selects 10%–15% of its counties (totaling 437 and 459 counties, respectively). Each county was stratified into five geographical sectors (east, west, south, north, and central) with one administrative village randomly selected per sector. From each village, 200 permanent residents were enrolled by cluster sampling, with 1,000 participants per county (*7–13*) representing all age groups. Each participant provided a fresh stool specimen (30 g).

Five households per village were randomly chosen for environmental sampling. One composite soil sample (≥400 g) was collected from each household's farmland or garden, subdivided for pathogen-specific analysis: 350 g for hookworm larval detection and 50 g for *Ascaris lumbricoides* egg identification.

Examination Methods

Fecal samples were analyzed for soil-transmitted helminth eggs using the modified Kato-Katz thick smear method, with duplicate slides per sample. Soil samples were processed for hookworm larvae via warm saline (5% NaCl, 45 °C) sedimentation and for *Ascaris lumbricoides* eggs via saturated sodium nitrate flotation.

Quality Control

The National Institute of Parasitic Diseases, Chinese Center for Disease Control and Prevention (National Center for Tropical Diseases Research), hereafter referred to as the National Institute of Parasitic Diseases (NIPD), delivers standardized training and on-site supervision. Provincial and municipal CDCs provided technical training and validated the results by reexamining 10% of positive and 5% of negative slides from each site. The NIPD also performed random slide rechecks.

All data were entered into the national Parasitic Disease Control Information Management System at the county level and subjected to multi-tier verification (municipal, provincial, and national). At each stage, discrepancies triggered the return and correction of data. The national authorities conducted a final review to obtain a definitive dataset.

Statistical Analysis

Data were analyzed using SAS 9.2 (SAS Institute Inc., Cary, NC, USA). Overall and species-specific (hookworm, *Ascaris lumbricoides*, *Trichuris trichiura*) infection rates and intensities were calculated, stratified by PLAD, sex, and age group, with between-group comparisons made by chi-square test (α =0.05). Soil detection rates for hookworm larvae and *Ascaris* eggs were also determined using the following formula:

$$\text{infection rate}(\%) = (\text{number of positive cases}/\text{number examined}) \times 100\% \quad (1)$$

$$\text{detection rate}(\%) = (\text{number of positive soil samples}/\text{number of soil samples examined}) \times 100\%. \quad (2)$$

RESULTS

Overall Prevalence of STH Infections

The STH infection rates in 2023 and 2024 were 0.53% (2,381/449,220) and 0.47% (2,233/476,756) respectively (Table 1). The infection rate is significantly lower in 2024 than in 2023 (χ^2=7.56; P<0.05).

Geographical Distribution

The STH infection rates in PLADs and XPCC demonstrated marked geographical heterogeneity, and the highest PLAD prevalence was recorded in Sichuan, Yunnan, and Chongqing in both years. No infections were detected in the four PLADs in 2023 or in eight PLADs in 2024 (Table 1).

Gender Distribution

Sex heterogeneity was observed in both years. The infection rate was significantly higher in women compared to men both in 2023 (χ^2=23.15, P<0.0001) and in 2024 (χ^2=6.87, P<0.01).

Age Distribution

Age group heterogeneity was found, with the highest infection rate observed in individuals aged 60 years and above, and the lowest in individuals aged 0–6 years in both years. Statistically significant differences in infection rates were identified among all age groups in

TABLE 1. Infection rate of soil-transmitted helminth by PLADs in China, 2023–2024.

PLADs	2023									2024								
	No. exam' d	STH		Hookworm		*Ascaris lumbricoides*		*Trichuris trichura*		No. exam' d	STH		Hookworm		*Ascaris lumbricoides*		*Trichuris trichura*	
		No. infected	Infection rate (%)	No. infected	Infection rate (%)	No. infected	Infection rate (%)	No. infected	Infection rate (%)		No. infected	Infection rate (%)	No. infected	Infection rate (%)	No. infected	Infection rate (%)	No. infected	Infection rate (%)
Beijing	7,376	0	0	0	0	0	0	0	0	7,377	0	0	0	0	0	0	0	0
Tianjin	3,041	0	0	0	0	0	0	0	0	3,094	0	0	0	0	0	0	0	0
Hebei	20,100	0	0	0	0	0	0	0	0	22,292	0	0	0	0	0	0	0	0
Shanxi	18,383	8	0.04	0	0	8	0.04	0	0	15,290	0	0	0	0	0	0	0	0
Inner Mongolia	10,096	1	0.01	0	0	1	0.01	0	0	16,101	0	0	0	0	0	0	0	0
Liaoning	14,016	7	0.05	0	0	7	0.05	0	0	14,003	9	0.06	0	0	9	0.06	0	0
Jilin	23,820	40	0.17	0	0	40	0.17	0	0	21,040	23	0.11	0	0	23	0.11	0	0
Heilongjiang	33,098	9	0.03	0	0	9	0.03	0	0	22,022	5	0.02	0	0	0	0	5	0.02
Shanghai	3,295	0	0	0	0	0	0	0	0	5,074	0	0	0	0	0	0	0	0
Jiangsu	11,279	2	0.02	1	0.01	0	0	1	0.01	11,254	5	0.04	4	0.04	1	0.01	0	0
Zhejiang	10,299	44	0.43	44	0.43	0	0	0	0	11,334	38	0.34	38	0.34	0	0	0	0
Anhui	29,168	103	0.35	89	0.31	6	0.02	9	0.03	29,214	76	0.26	62	0.21	8	0.03	7	0.02
Fujian	16,424	88	0.54	68	0.41	0	0	20	0.12	12,686	36	0.28	33	0.26	0	0	3	0.02
Jiangxi	15,295	110	0.72	84	0.55	23	0.15	3	0.02	15,303	70	0.46	51	0.33	7	0.05	12	0.08
Shandong	14,507	45	0.31	0	0	2	0.01	43	0.3	17,718	21	0.12	0	0	1	0.01	20	0.11
Henan	17,615	8	0.05	1	0.01	5	0.03	2	0.01	16,361	1	0.01	1	0.01	0	0	0	0
Hubei	13,218	7	0.05	0	0	5	0.04	2	0.02	11,184	0	0	0	0	0	0	0	0
Hunan	14,045	68	0.48	58	0.41	7	0.05	5	0.04	21,140	125	0.59	57	0.27	53	0.25	15	0.07
Guangdong	22,640	20	0.09	14	0.06	1	0	5	0.02	25,409	18	0.07	7	0.03	6	0.02	5	0.02
Guangxi	15,295	92	0.6	70	0.46	0	0	22	0.14	23,749	75	0.32	36	0.15	0	0	41	0.17
Hainan	4,177	26	0.62	22	0.53	0	0	4	0.1	3,009	28	0.93	27	0.9	0	0	1	0.03
Chongqing	9,069	258	2.84	220	2.43	34	0.37	4	0.04	8,516	233	2.74	194	2.28	32	0.38	9	0.11
Sichuan	17,288	631	3.65	276	1.6	178	1.03	249	1.44	34,052	719	2.11	466	1.37	90	0.26	214	0.63
Guizhou	16,260	72	0.44	52	0.32	18	0.11	4	0.02	20,228	69	0.34	46	0.23	15	0.07	8	0.04
Yunnan	19,966	593	2.97	412	2.06	116	0.58	82	0.41	17,554	480	2.73	434	2.47	9	0.05	45	0.26
Xizang	9,449	7	0.07	0	0	6	0.06	1	0.01	8,735	122	1.4	0	0	50	0.57	73	0.84
Shaanxi	19,071	3	0.02	0	0	3	0.02	0	0	20,014	0	0	0	0	0	0	0	0

Continued

PLADs	2023									2024								
	No. exam' d	STH		Hookworm		*Ascaris lumbricoides*		*Trichuris trichura*		No. exam' d	STH		Hookworm		*Ascaris lumbricoides*		*Trichuris trichura*	
		No. infected	Infection rate (%)	No. infected	Infection rate (%)	No. infected	Infection rate (%)	No. infected	Infection rate (%)		No. infected	Infection rate (%)	No. infected	Infection rate (%)	No. infected	Infection rate (%)	No. infected	Infection rate (%)
Gansu	10,228	3	0.03	0	0	3	0.03	0	0	10,453	20	0.19	0	0	20	0.19	0	0
Qinghai	6,252	87	1.39	0	0	87	1.39	0	0	6,142	32	0.52	0	0	32	0.52	0	0
Ningxia	9,277	22	0.24	0	0	20	0.22	2	0.02	10,357	15	0.14	0	0	15	0.14	0	0
Xinjiang	13,133	13	0.1	2	0.02	11	0.08	0	0	14,051	6	0.04	0	0	5	0.04	1	0.01
XPCC	2,040	14	0.69	0	0	13	0.64	1	0.05	2,000	7	0.35	0	0	7	0.35	0	0
Total	449,220	2,381	0.53	1413	0.31	603	0.13	459	0.1	476,756	2,233	0.47	1,456	0.31	383	0.08	459	0.1

Abbreviation: PLAD=provincial-level divisions; STH=soil-transmitted helminths; XPCC=Xinjiang Production and Construction Corps.

TABLE 2. Infection rate of soil-transmitted helminth by age group in China, 2023–2024.

Age groups (years)	2023									2024								
	No. exam' d	STH		Hookworm		*Ascaris lumbricoides*		*Trichuris trichura*		No. exam' d	STH		Hookworm		*Ascaris lumbricoides*		*Trichuris trichura*	
		No. infected	Infection rate (%)	No. infected	Infection rate (%)	No. infected	Infection rate (%)	No. infected	Infection rate (%)		No. infected	Infection rate (%)	No. infected	Infection rate (%)	No. infected	Infection rate (%)	No. infected	Infection rate (%)
0–6	28,354	73	0.26	6	0.02	45	0.16	28	0.10	27,416	35	0.13	12	0.04	17	0.06	8	0.03
7–14	55,754	309	0.55	68	0.12	145	0.26	137	0.25	54,484	200	0.37	22	0.04	60	0.11	151	0.28
15–44	123,008	415	0.34	165	0.13	124	0.10	147	0.12	124,151	381	0.31	182	0.15	77	0.06	138	0.11
45–59	111,270	508	0.46	312	0.28	129	0.12	78	0.07	116,599	505	0.43	334	0.29	91	0.08	90	0.08
≥60	130,834	1,076	0.82	862	0.66	160	0.12	69	0.05	154,106	1,112	0.72	906	0.59	138	0.09	72	0.05
Total	449,220	2,381	0.53	1,413	0.31	603	0.13	459	0.10	476,756	2,233	0.47	1,456	0.31	383	0.08	459	0.10

Abbreviation: STH=soil-transmitted helminths.

2023 (χ^2=350.72, P<0.0001) and 2024 (χ^2=364.77, P<0.0001) (Table 2).

Hookworm Infection

The overall hookworm infection rate was 0.31% (1,413/449,220) and 0.31% (1,456/476,756) in 2023 and 2024 respectively, and no significant difference was found (χ^2=0.63, P>0.05) between them. The infection rates exceeded 1.00% in three PLADs – Chongqing, Yunnan, and Sichuan – in both years. No infections were detected in 16 PLADs in 2023 or 17 PLADs in 2024 (Table 1). Moreover, sex and age differences were statistically significant in both years (P<0.001) (Table 2).

Ascaris lumbricoides Infection

The overall infection rate of *Ascaris lumbricoides* was 0.13% (603/449,220) in 2023 and 0.08% (383/476,756) in 2024, the infection rate was higher in 2023 than in 2024 (χ^2=63.17, P<0.001). Rates were above 1.00% in two PLADs by 2023 and in no PLADs by 2024. No infections were detected in 9 PLADs in 2023 and in 14 PLADs in 2024 (Table 1). Moreover, sex and age differences were statistically significant in both years (P<0.001), except for sex, which showed no statistical significance in 2023 (P>0.05) (Table 2).

Trichuris trichiura Infection

The overall *Trichuris trichiura* infection rate was 0.10% (459/449,220) in 2023 and 0.10% (459/476,756) in 2024 respectively, and no significant difference was found (χ^2=0.81, P>0.05) between them. The prevalence was <1.00% in all PLADs in both years, except Sichuan in 2023. No infections were detected in 14 PLADs in 2023 or in 17 PLADs in 2024 (Table 1). No significant sex differences were observed in either year (P>0.05), while age differences were statistically significant in both years (P<0.0001) (Table 2).

Infection Intensity

Over 85% and 93% of hookworm, *Ascaris lumbricoides*, and *Trichuris trichiura* infections were mild in 2023 and 2024, respectively. Moderate and severe cases were observed in all three species in both years (Table 3).

Soil Contamination

The detection rates of Ascaris eggs were 1.93% (52/2700) and 1.37% (37/2,691) in soil samples, and positive samples were identified in nine and four PLADs in 2023 and 2024, respectively. The highest detection rates were found in Qinghai and Sichuan in both years, and contamination was found in both farmland and vegetable garden soils.

The detection rates of hookworm larvae were 2.44% (66/2,700) and 2.27% (61/2,691) in the soil samples, respectively, and positive samples were identified in seven and five PLADs in 2023 and 2024, respectively. The highest detection rates were observed in Jiangxi and Anhui in 2023 and in Yunnan and Chongqing in 2024, and larvae were present in both farmland and vegetable garden soils.

DISCUSSION

Soil-transmitted helminthiasis remains a persistent public health challenge that has long been endemic to China (*14*). Since the 20th century, nationwide control efforts have made substantial progress. Successive national parasite surveys demonstrated a marked decline in STH infection rates from 53.58% in 1990 (*4*) to 4.49% in 2015 (*6*). Despite this reduction, transmission continues, with pockets of hyper-endemicity highlighting control complexity (*15*). The National Implementation Plan for Comprehensive Control of Key Parasitic Diseases (2024–2030) calls for enhanced and control targets: highly endemic PLADs should reduce infection rates by >10% by 2025 and by >30% by 2030, while other PLADs maintain low prevalence. Sustained, intensive interventions are crucial to improve STH control in China.

A national STH surveillance system currently covers over 400 monitoring counties across all 31 PLADs and XPCC (*7*). Surveillance data from 2016 to 2022 indicate a steady infection rate decline from 2.46% to 0.64% (*7–13*). New data show rates of 0.53% (2023) and 0.47% (2024), continuing the downward trend, highlighting persistent epidemiological patterns. Infections were clustered regionally, with higher prevalence in warm, humid southern PLADs (Sichuan, Yunnan, and Chongqing), where climate and agricultural practices favor transmission, particularly of hookworm (*15*). Lower rates occurred in cooler, more developed eastern and northeastern regions (Beijing, Shanghai, and Heilongjiang). Demographically, infection rates were higher in women and peaked among adults ≥60 years, followed by children aged 7–14 years and adults 45–59 years, consistent with known at-risk populations (*7–13*). Older adults

TABLE 3. Infection intensity of hookworm, *Ascaris lumbricoides*, and *Trichuris trichiura* in China, 2023–2024.

Species	2023						2024					
	No. infected			Ratio of infection (%)			No. infected			Ratio of infection (%)		
	Mild	Moderate	Severe	Mild	Moderate	Severe	Mild	Moderate	Severe	Mild	Moderate	Severe
Hookworm	1,324	41	48	93.70	2.90	3.40	1,371	42	43	94.16	2.88	2.95
Ascaris lumbricoides	516	86	1	85.57	14.26	0.17	371	10	2	96.87	2.61	0.52
Trichuris trichiura	439	19	1	95.64	4.14	0.22	431	28	0	93.90	6.10	0

frequently face farming; children face risks from outdoor activities and hygiene practices. Given hookworm dominance, future strategies should prioritize this species while maintaining comprehensive efforts against all major STH.

Surveillance data showed persistent *Ascaris* egg contamination in PLADs (Qinghai and Sichuan), and with hookworm larvae in various regions (Jiangxi and Yunnan), indicating ongoing environmental transmission risk. Future STH control should prioritize sanitation improvements, such as expanding access to hygienic toilets and enhancing environmental management, to disrupt transmission and lower infection rates.

Given geographical disparities, regionally targeted strategies are required. In highly endemic areas, focused interventions should aim to reduce infection rates, and a comprehensive strategy of health education as the precursor and source control as the mainstay should be implemented. In low-endemic areas, efforts should shift toward transmission control and eventual elimination. Currently, STH infection rates exceed 1.00% in only four PLADs, whereas all others remain below this threshold. Specific provincial objectives for transmission control and interruption were set in line with the National Implementation Plan for Comprehensive Control of Key Parasitic Diseases (2024–2030). PLADs are advised to align activities with the national standard Control and Interruption of Soil-transmitted Helminth Transmission (WS/T629-2018) and to utilize the forthcoming Measures of Evaluation for Soil-transmitted Helminth Transmission Control and Interruption to systematically advance toward STH control and eventual interruption in China.

China has made significant strides in soil-transmitted helminthiasis prevention and control, where the National Surveillance System plays a key role. Currently, the national prevalence is low. However, considerable disparities persist across regions and population groups, with some areas reporting elevated infection rates. Therefore, implementing targeted interventions in high-prevalence regions guided by national surveillance results is essential. In areas where conditions allow, efforts should be made to control and eliminate soil-transmitted helminthiasis, advancing China's efforts towards a new phase of parasitic disease control.

Conflicts of interest: No conflicts of interest.

Acknowledgements: Appreciation goes to all surveillance personnel at provincial, municipal, and county levels of the Disease control agencies across all 31 provinces (autonomous regions, municipalities) and the Xinjiang Production and Construction Corps for their dedicated efforts in the National Soil-transmitted Helminth Surveillance Program.

Ethical statement: This study used surveillance data from the National Institute of Parasitic Diseases (NIPD), Chinese Center for Disease Control and Prevention (China CDC). Ethical approval was granted by the Institutional Ethical Review Committee of NIPD, China CDC (Nos. 2021006 in 2023 and 2022001 in 2024). No personally identifiable information is disclosed. Oral informed consent was obtained from all participants and their guardians provided consent for those under 18 years of age.

Funding: This work was funded by the National Health Commission of China.

doi: 10.46234/ccdcw2026.088

[#] Corresponding authors: Shizhu Li, lisz@chinacdc.cn; Menbao Qian, qianmb@nipd.chinacdc.cn.

[1] National Health Commission Key Laboratory of Parasite and Vector Biology, WHO Collaborating Centre for Tropical Diseases, National Center for International Research on Tropical Diseases, National Institute of Parasitic Diseases, Chinese Center for Disease Control and Prevention & Chinese Center for Tropical Diseases Research, Shanghai, China; [2] School of Global Health, School of Medicine, Chinese Center for Tropical Diseases Research-Shanghai Jiao Tong University, Shanghai, China.

Submitted: January 08, 2026
Accepted: March 26, 2026
Issued: May 01, 2026

REFERENCES

1. Bethony J, Brooker S, Albonico M, Geiger SM, Loukas A, Diemert D, et al. Soil-transmitted helminth infections: ascariasis, trichuriasis, and hookworm. Lancet 2006;367(9521):1521 – 32. https://doi.org/10.1016/S0140-6736(06)68653-4.
2. Caldrer S, Ursini T, Santucci B, Motta L, Angheben A. Soil-transmitted helminths and anaemia: a neglected association outside the tropics. Microorganisms 2022;10(5):1027. https://doi.org/10.3390/microorganisms10051027.
3. Ellwanger JH, Ziliotto M, Kulmann-Leal B, Chies JAB. Iron deficiency and soil-transmitted helminth infection: classic and neglected connections. Parasitol Res 2022;121(12):3381 – 92. https://doi.org/10.1007/s00436-022-07697-z.
4. Xu LQ, Jiang ZX, Yu SH, Xu SH, Chang J, Wu ZX, et al. Characteristics and recent trends in endemicity of human parasitic diseases in China. Chin J Parasitol Parasit Dis 1995;13(3):214-7. (In Chinese).
5. Coordinating Office of the National Survey on the Important Human Parasitic Diseases. A national survey on current status of the important parasitic diseases in human population. Chin J Parasitol Parasit Dis 2005;23(5 Suppl):332-40. http://dx.doi.org/10.3969/j.issn.1000-7423.2005.z1.004. (In Chinese).
6. Chen YD, Zhou CH, Zhu HH, Huang JL, Duan L, Zhu TJ, et al. National survey on the current status of important human parasitic diseases in China in 2015. Chin J Parasitol Parasit Dis 2020;38(1):5 – 16. https://doi.org/10.12140/j.issn.1000-7423.2020.01.002.
7. Chinese Center for Disease Control and Prevention. Annual report on surveillance of infectious diseases in China, 2016. Beijing: Chinese Center for Disease Control and Prevention. 2016; p. 384-392. https://book.kongfz.com/22528/7161116072/. (In Chinese).
8. Zhu HH, Huang JL, Zhu TJ, Duan L, Zhou CH, Qian MB, et al. National surveillance of soil-transmitted helminth infections in 2017. Chin J Parasitol Parasit Dis 2019;37(1):12 – 7. https://doi.org/10.12140/j.issn.1000-7423.2019.01.003.
9. Zhu HH, Huang JL, Zhou CH, Zhu TJ, Qian MB, Zhang MZ, et al. Soil-transmitted helminthiasis—China, 2018. China CDC Wkly 2020;2(3):34 – 8. https://doi.org/10.46234/ccdcw2020.010.
10. Zhu HH, Huang JL, Chen YD, Zhou CH, Zhu TJ, Qian MB, et al. Analysis on endemic status of soil-transmitted nematode infection in China in 2019. Chin J Parasitol Parasit Dis 2021;39(5):666 – 73. https://doi.org/10.12140/j.issn.1000-7423.2021.05.015.
11. Zhang MZ, Huang JL, Zhu HH, Zhou CH, Zhu TJ, Qian MB, et al. Epidemiological analysis of soil-transmitted nematode infections in China in 2020. Chin J Parasitol Parasit Dis 2023;41(3):331 – 5,343. https://doi.org/10.12140/j.issn.1000-7423.2023.03.011.
12. Zhao LY, Huang JL, Zhou CH, Zhu TJ, Zhu HH, Zhou XN, et al. National surveillance on soil-transmitted helminth infections in China, 2021. Chin J Parasitol Parasit Dis 2024;42(6):687 – 93. https://doi.org/10.12140/j.issn.1000-7423.2024.06.001.
13. Zhu HH, Huang JL, Zhou CH, Zhu TJ, Zhao LY, Qian MB, et al. National surveillance of soil-transmitted helminth infecions in China in 2022. Chin J Parasitol Parasit Dis 2025;43(4):451 – 7. https://doi.org/10.12140/j.issn.1000-7423.2025.04.001.
14. Tang LH, Xu LQ, Chen YD. Parasitic disease control and research in China. Beijing: Beijing Science and Technology Press. 2012; p. 2. http://find.nlc.cn/search/showDocDetails?docId=3389715174287262016&dataSource=ucs01&query. (In Chinese).
15. Zhu HH, Zhou CH, Zhang MZ, Huang JL, Zhu TJ, Qian MB, et al. Engagement of the National Institute of Parasitic Diseases in control of soil-transmitted helminthiasis in China. Adv Parasitol 2020;110:217 – 44. https://doi.org/10.1016/bs.apar.2020.04.008.

Vital Surveillances

Comparative Epidemiology and Transmission Risk Assessment of Imported and Indigenous Dengue Fever at the National and Selected Provincial Levels, China, 2005–2025

Sihan Li[1]; Meilan Huang[2]; Qian Ren[1]; Yanping Zhang[1]; Qiulan Chen[1,#]

ABSTRACT

Introduction: This study compared epidemiological characteristics of imported and indigenous dengue fever cases in China from 2005 to 2025 and assessed the dynamic provincial transmission risks.

Methods: This study compared the 21-year trends in national surveillance data. It examined temporal changes in the countries of origin of imported cases and the dynamic risk ratio of indigenous to imported cases across ten high-import provinces, as well as the disparity of epidemiological characteristics between imported and indigenous cases.

Results: Indigenous cases dominated the epidemic in China (90.1%, 134,129/148,893). Imported cases (9.9%, 14,764/148,893) were the initial trigger, increasing notably before the local epidemic season. They were predominantly men (70.5%) aged 25–49 years, mainly "farmers and workers (38.6%)" and "commercial/service personnel (22.9%)". In contrast, indigenous cases had a balanced sex ratio (1.1:1), and "household/unemployed/retired persons (32.1%)" constituted the largest occupational group. Further spatiotemporal analysis revealed that: 1) The primary source country for imported cases nationwide shifted from Cambodia (41.1%) to Myanmar (29.6%); 2) Imported cases in Yunnan were predominantly from Myanmar (71.1%) and "farmers and workers (50.5%)", whereas in Guangdong, they were more diverse in origin and dominated by "commercial/service personnel (30.2%)"; 3) The risk ratio of indigenous to imported cases across ten provinces exhibited significant heterogeneity: Yunnan and Guangdong were persistent high-risk areas, whereas Sichuan and Jiangsu maintained lower risk. Hunan and Chongqing exhibited high-risk in recent years, with Chongqing's ratio reaching 36.5 in 2025 and Hunan's 15.5 in 2024.

Conclusions: The dengue fever epidemic in China was initiated by importation; however, the scale and risk of subsequent local transmission varied significantly and dynamically across provinces. Control strategies should integrate source interception of imported cases with tailored interventions addressing distinct importation profiles, evolving local transmission risks, and population characteristics across provinces.

Dengue fever (DF) has increased sharply worldwide, with cases increasing from 0.5 million in 2000 to 5.2 million in 2019 (*1–2*). In 2024, the number of reported cases surged to 14.4 million, with 11,000 deaths worldwide. Southeast Asia and the Western Pacific region bear the highest burden of severe cases and fatality rates, respectively, imposing a substantial public health burden (*2–4*).

Southeast Asia remains the primary source of imported dengue fever cases into China, and imported cases have repeatedly triggered large local outbreaks (*5–6*). The geographical scope of local transmission has expanded northward, affecting 28 provincial-level administrative divisions, 217 cities, and 895 counties by 2024, highlighting a growing public health challenge (*5–6*). However, comparative analyses of the epidemiological characteristics of imported and indigenous dengue fever cases nationwide are relatively scarce, particularly lacking the latest data following the coronavirus disease 2019 (COVID-19) pandemic (*5–10*). There is a notable lack of quantitative analyses assessing the importation-transmission risk across provinces and phases, as well as the origin counties of imported cases (*5–11*).

Therefore, based on the latest national surveillance data spanning 21 years (2005–2025), this study systematically analyzes differences between imported and indigenous cases in terms of seasonality, geographical distribution, and population distribution.

It further quantifies the import-transmission risk ratios and their dynamic changes across different provinces and compares the dynamic differences of origin countries at the national and subnational levels, aiming to identify high-risk provinces and populations. These findings will provide evidence for the formulation of targeted region-specific prevention and control strategies in China.

METHODS

Data Sources

Dengue fever case data were obtained from the National Notifiable Disease Reporting System (NNDRS), including cases reported by 31 provincial-level administrative divisions (PLADs) and the Xinjiang Production and Construction Corp (XPCC). The case data included demographic, clinical, and temporal variables. This study primarily conducted a comparative analysis of imported and local cases in Chinese PLADs.

Case Definitions

Dengue fever cases were defined according to the *Diagnostic Criteria for Dengue Fever (WS 216-2018)* (*12*). Both clinically diagnosed and laboratory-confirmed cases reported in China between January 1, 2005, and December 31, 2025, were included. Imported dengue fever cases (*13*) were defined as cases in individuals with a history of travel to dengue-endemic countries or regions within 14 days before symptom onset, for which local infections were excluded through epidemiological investigation. Indigenous dengue fever cases (*13*) were defined as those occurring in individuals who had resided in China during the 14 days prior to symptom onset and had no history of international travel. Indigenous cases included both intra- and inter-provincial transmission.

Statistical Analysis

The temporal, spatial, and population distributions of imported and indigenous dengue fever cases, as well as the source countries of imported cases in China and in the two high-burden PLADs of Guangdong and Yunnan from 2005 to 2025, were analyzed. The normality of continuous variables was assessed prior to analysis. Normally distributed data are presented as the mean ± standard deviation, while non-normally distributed data are summarized as median and interquartile range (IQR). Inter-group comparisons were conducted using appropriate non-parametric tests. Categorical data were computed as frequency (percentage) and compared using the chi-square test, with the significance level set at $\alpha = 0.05$. The transmission risk ratio of indigenous to imported cases was calculated for the 10 PLADs with the highest number of imported cases. A higher ratio indicates a greater number of indigenous cases relative to the given number of imported infections, corresponding to an elevated relative risk of local transmission. Microsoft Excel 2019 was used for data management and visualization. SPSS (version 27.0.1, IBM Corp, Armonk, New York, United States) was used to perform inter-group comparisons. R (version 4.3.3, Vienna University of Economics and Business, Vienna, Austria) was used to illustrate changes in the proportions of infection sources.

RESULTS

General Characteristics

Overall epidemic trend with major peaks. The number of dengue cases reported annually in China fluctuated significantly over the 21-year period, characterized by two distinct high-incidence cycles. Following a low-incidence phase (2005–2012, mostly <600 cases annually), the first major epidemic occurred in 2014, with a peak of 46,864 cases (Figure 1A). After a period of moderate fluctuations, a second epidemic cycle began in 2019 (22,188 cases), culminating in a second historical peak of 24,278 cases by 2024. The incidence dropped sharply in 2020–2021 (778 and 41 cases, respectively) owing to the COVID-19 pandemic before rebounding significantly from 2022 onward.

Overall composition and dominance of indigenous transmission. Between 2005 and 2025, a total of 148,893 dengue fever cases were reported in China. Of these, 134,129 (90.1%) cases were indigenous, whereas 14,764 (9.9%) were imported (Figure 1A, Supplementary Table S1, available at http://weekly.chinacdc.cn/). The epidemic was predominantly driven by indigenous transmission, with the annual reported numbers ranging from 10 to 46,605 during this long period (Figure 1B). In contrast, imported cases served as the initial trigger and maintained baseline presence (Figure 1A–1C, Supplementary Table S1).

Seasonality Difference in Imported and Indigenous Cases

Pronounced seasonal epidemic peaks. Indigenous

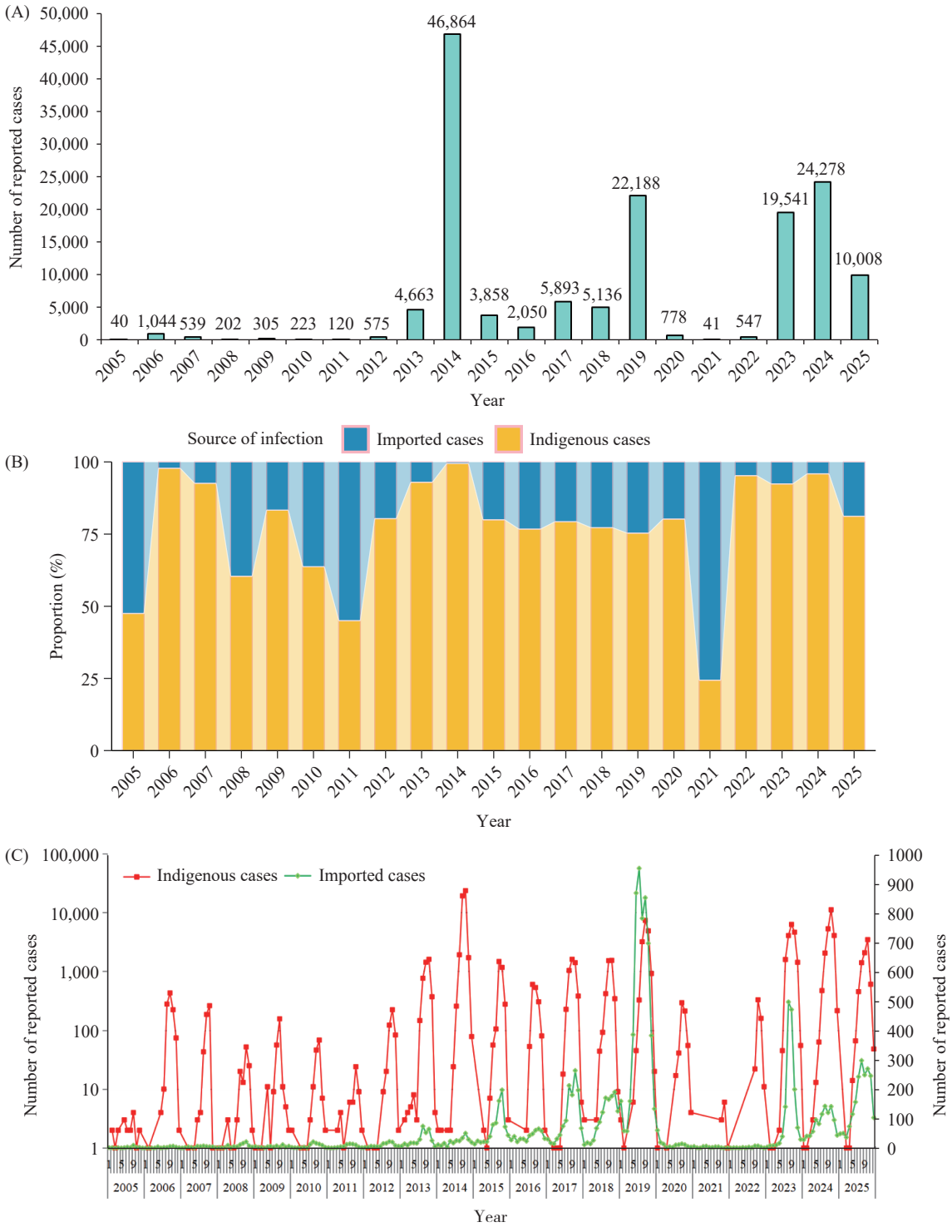

FIGURE 1. Temporal trends of reported dengue fever cases in China. (A) Number of reported cases; (B) Percentage of infection sources; (C) Monthly distribution of reported cases.

cases peaked sharply in late summer and autumn. August, September, and October accounted for 118,885 cases (Supplementary Table S1). October accounted for 54,966 cases (41.0%), transmission was minimal from December to June (only 0.7% of the total indigenous cases).

Role of imported cases in initiating outbreaks. Imported cases occurred throughout the year but showed distinct peaks. The number of imported cases began to increase in May (848) and June (1,433),

before the local epidemic surge (Supplementary Table S1). The highest numbers were recorded in August (2,423) and September (2,452). This pattern suggests that imported cases, which increase ahead of the local transmission season, are key drivers seeding local outbreaks.

Monthly shift in case-type dominance. The monthly composition ratios of case types demonstrated a clear seasonal cycle. Imported cases were predominant from December to June, constituting over 95% of cases from January to April. A pivotal shift occurred in July, when indigenous cases outnumbered imported cases (Supplementary Table S1). Indigenous cases dominated the peak period from August to October, comprising 86.8%, 95.1%, and 96.1% of cases, respectively. By December, the pattern had reverted, with imported cases exceeding indigenous cases (Figure 1C, Supplementary Table S1).

Regional Distribution of Imported and Indigenous Cases

The number of PLADs reporting indigenous cases increased from 8 in 2005 to 27 in 2023. From 2005 to 2025, Guangdong accounted for the highest number of indigenous cases (86,566), followed by Yunnan (28,771), Guangxi (4,179), Chongqing (3,402), Fujian (2,683), and Zhejiang (2,402) (Supplementary Table S2, available at http://weekly.chinacdc.cn/). However, from 2019 to 2023, Yunnan reported significantly more indigenous cases than other PLADs, ranking first. From 2005 to 2018, Chongqing reported no more than 10 indigenous cases annually, but this number surged sharply to 1,269 in 2019 and 1,973 in 2025.

In 2005, China reported imported dengue cases in 8 PLADs; by 2019, this had increased to 29 PLADs. By 2025, all 31 PLADs in China reported imported dengue cases, ranging from 1 to 4,173. The highest number of imported cases was recorded in Yunnan at 4,173 (28.3%) (Supplementary Table S2).

Dynamics of Source Countries at National and Subnational Levels

National-level composition and trends. In 2005, imported cases originated from nine different countries or regions and had expanded to 52 countries by 2025. The majority of imported cases (87.1%) were from Southeast Asian countries, with Cambodia (29.1%), Myanmar (24.3%), and Thailand (8.0%) being the predominant source countries (Table 1). The composition shifted over time: the proportion from Southeast Asia was 79.1% during 2005–2009, decreased slightly to 76.2% in 2010–2014, peaked at 89.0% in 2015–2019 (driven by a surge from Cambodia, 41.1%), and reached 85.8% in 2020–2024, with Myanmar, Laos, and Cambodia becoming the leading sources (Table 1).

Yunnan Province: high concentration from Myanmar. Yunnan Province reported 4,173 imported cases, with an even higher concentration from Southeast Asia (3,979, 95.4%) (Table 2). Myanmar was the dominant source (72.4%), followed by Laos (10.3%) and Cambodia (6.9%). This concentration intensified over time: Myanmar's contribution rose from 60.0% to 67.5% (2005–2019), before peaking at 80.9% in 2020–2025. Concurrently, the overall share of Southeast Asian sources increased from 86.0% to 99.0% in the most recent period (Table 2).

Guangdong Province: dynamic shifts in major sources. Guangdong Province documented 2,960 imported cases, of which 2,512 cases (84.9%) originated from Southeast Asia. Cambodia (37.4%), Thailand (13.3%), and Malaysia (8.9%) were the main sources (Table 3). The primary source countries varied significantly by period: Thailand and Indonesia led in 2005–2009; Thailand led in 2010–2014; Cambodia dominated in 2015–2019; while in 2020–2025, sources diversified, with Thailand and Indonesia becoming primary sources and Cambodia's share falling (Table 3).

Transmission Risk Ratio

Overall trends. The indigenous-to-imported risk ratio, defined as the number of indigenous cases per imported case, was analyzed for ten Chinese provinces from 2005 to 2025. This ratio reflects the relative risk of local outbreaks following importation. Over the 21-year study period, the risk ratios exhibited significant annual and periodic fluctuations. Extreme peaks indicate years of intense local transmission, such as Yunnan Province in 2022 (ratio: 86.3), Guangdong Province in 2024 (81.1), and Chongqing Municipality in 2025 (36.5) (Figure 2). In contrast, a risk ratio below 1.0, common across many PLADs and years, signified the predominance of imported cases with minimal local spread (Figure 2).

PLADs with persistent high risk. Yunnan and Guangdong Provinces were identified as persistently high-risk areas. Yunnan maintained elevated risk ratios (2.0–5.0) from 2014 to 2019, with a peak of 86.3 in 2022. Guangdong exhibited a bimodal pattern, with a peak in 2015 (11.3) and a larger one in 2023 (37.9)

TABLE 1. Distribution of countries of origin of imported dengue cases in China, 2005 to 2025.

Source country	Total, *n* (%)	2005–2009, *n* (%)	2010–2014, *n* (%)	2015–2019, *n* (%)	2020–2025, *n* (%)
Southeast Asian countries	12,863 (87.1)	170 (79.1)	645 (76.2)	8,111 (89.0)	3,937 (85.8)
Cambodia	4,294 (29.1)	18 (8.4)	21 (2.5)	3,744 (41.1)	511 (11.1)
Myanmar	3,582 (24.3)	37 (17.2)	156 (18.4)	2,033 (22.3)	1,356 (29.6)
Thailand	1,187 (8.0)	17 (7.9)	127 (15.0)	697 (7.6)	346 (7.5)
Indonesia	917 (6.2)	25 (11.6)	71 (8.4)	214 (2.3)	607 (13.2)
Laos	828 (5.6)	8 (3.7)	73 (8.6)	240 (2.6)	507 (11.1)
Philippines	675 (4.6)	19 (8.8)	81 (9.6)	421 (4.6)	154 (3.4)
Malaysia	672 (4.6)	8 (3.7)	80 (9.4)	378 (4.1)	206 (4.5)
Vietnam	548 (3.7)	24 (11.2)	17 (2.0)	323 (3.5)	184 (4.0)
Singapore	160 (1.1)	14 (6.5)	19 (2.2)	61 (0.7)	66 (1.4)
Non-southeast Asian countries	1,901 (12.9)	45 (20.9)	202 (23.8)	1,005 (11.0)	649 (14.2)
Maldives	313 (2.1)	1 (0.5)	11 (1.3)	124 (1.4)	177 (3.9)
India	277 (1.9)	13 (6.0)	55 (6.5)	196 (2.2)	13 (0.3)
Bangladesh	171 (1.2)	6 (2.8)	16 (1.9)	74 (0.8)	75 (1.6)
Sri Lanka	171 (1.2)	1 (0.5)	6 (0.7)	124 (1.4)	40 (0.9)
Angola	73 (0.5)	1 (0.5)	28 (3.3)	29 (0.3)	15 (0.3)
Papua New Guinea	56 (0.4)	0 (0.0)	5 (0.6)	38 (0.4)	13 (0.3)
Pakistan	42 (0.3)	0 (0.0)	0 (0.0)	24 (0.3)	18 (0.4)
Tanzania	42 (0.3)	0 (0.0)	3 (0.4)	12 (0.1)	27 (0.6)
Other countries	756 (5.1)	23 (10.7)	78 (9.2)	384 (4.2)	271 (5.9)
Total	14,764 (100.0)	215 (100.0)	847 (100.0)	9,116 (100.0)	4,586 (100.0)

TABLE 2. Distribution of countries of origin of imported dengue cases in Yunnan Province, 2005 to 2025.

Source country	Total, *n* (%)	2005–2009, *n* (%)	2010–2014, *n* (%)	2015–2019, *n* (%)	2020–2025, *n* (%)
Southeast Asian countries	3,979 (95.4)	43 (86.0)	174 (88.8)	2,158 (93.5)	1,604 (99.0)
Myanmar	3,020 (72.4)	30 (60.0)	123 (62.8)	1,557 (67.5)	1,310 (80.9)
Laos	431 (10.3)	7 (14.0)	37 (18.9)	142 (6.2)	245 (15.1)
Cambodia	286 (6.9)	1 (2.0)	0 (0.0)	272 (11.8)	13 (0.8)
Thailand	113 (2.7)	0 (0.0)	13 (6.6)	78 (3.4)	22 (1.4)
Vietnam	52 (1.2)	5 (10.0)	0 (0.0)	43 (1.9)	4 (0.2)
Malaysia	36 (0.9)	0 (0.0)	1 (0.5)	35 (1.5)	0 (0.0)
Philippines	26 (0.6)	0 (0.0)	0 (0.0)	25 (1.1)	1 (0.1)
Indonesia	13 (0.3)	0 (0.0)	0 (0.0)	4 (0.2)	9 (0.6)
Singapore	2 (0.0)	0 (0.0)	0 (0.0)	2 (0.1)	0 (0.0)
Non-southeast Asian countries	194 (4.6)	7 (14.0)	22 (11.2)	149 (6.5)	16 (1.0)
India	29 (0.7)	0 (0.0)	3 (1.5)	26 (1.1)	0 (0.0)
Sri Lanka	21 (0.5)	0 (0.0)	0 (0.0)	20 (0.9)	1 (0.1)
Bangladesh	12 (0.3)	0 (0.0)	0 (0.0)	9 (0.4)	3 (0.2)
Maldives	10 (0.2)	0 (0.0)	0 (0.0)	8 (0.3)	2 (0.1)
Other countries	122 (2.9)	7 (14.0)	19 (9.7)	86 (3.7)	10 (0.6)
Total	4,173 (100.0)	50 (100.0)	196 (100.0)	2,307 (100.0)	1,620 (100.0)

TABLE 3. Distribution of countries of origin of imported dengue cases in Guangdong Province, 2005 to 2025.

Source country	Total, *n* (%)	2005–2009, *n* (%)	2010–2014, *n* (%)	2015–2019, *n* (%)	2020–2025, *n* (%)
Southeast Asian countries	2,512 (84.9)	41 (75.9)	179 (81.7)	1,720 (88.4)	572 (77.1)
Cambodia	1,107 (37.4)	4 (7.4)	9 (4.1)	974 (50.1)	120 (16.2)
Thailand	395 (13.3)	12 (22.2)	59 (26.9)	215 (11.1)	109 (14.7)
Malaysia	263 (8.9)	1 (1.9)	38 (17.4)	137 (7.0)	87 (11.7)
Indonesia	197 (6.7)	11 (20.4)	21 (9.6)	63 (3.2)	102 (13.7)
Vietnam	182 (6.1)	6 (11.1)	10 (4.6)	103 (5.3)	63 (8.5)
Myanmar	142 (4.8)	1 (1.9)	11 (5.0)	113 (5.8)	17 (2.3)
Philippines	128 (4.3)	3 (5.6)	15 (6.8)	84 (4.3)	26 (3.5)
Laos	59 (2.0)	0 (0.0)	9 (4.1)	17 (0.9)	33 (4.4)
Singapore	39 (1.3)	3 (5.6)	7 (3.2)	14 (0.7)	15 (2.0)
Non-southeast Asian countries	448 (15.1)	13 (24.1)	40 (18.3)	225 (11.6)	170 (22.9)
India	98 (3.3)	7 (13.0)	14 (6.4)	69 (3.5)	8 (1.1)
Maldives	59 (2.0)	0 (0.0)	4 (1.8)	21 (1.1)	34 (4.6)
Sri Lanka	58 (2.0)	0 (0.0)	4 (1.8)	36 (1.9)	18 (2.4)
Bangladesh	52 (1.8)	3 (5.6)	8 (3.7)	16 (0.8)	25 (3.4)
Pakistan	12 (0.4)	0 (0.0)	0 (0.0)	7 (0.4)	5 (0.7)
Tanzania	12 (0.4)	0 (0.0)	0 (0.0)	3 (0.2)	9 (1.2)
The United Arab Emirates	11 (0.4)	0 (0.0)	0 (0.0)	0 (0.0)	11 (1.5)
Other countries	146 (4.9)	3 (5.6)	10 (4.6)	73 (3.8)	60 (8.1)
Total	2,960 (100.0)	54 (100.0)	219 (100.0)	1,945 (100.0)	742 (100.0)

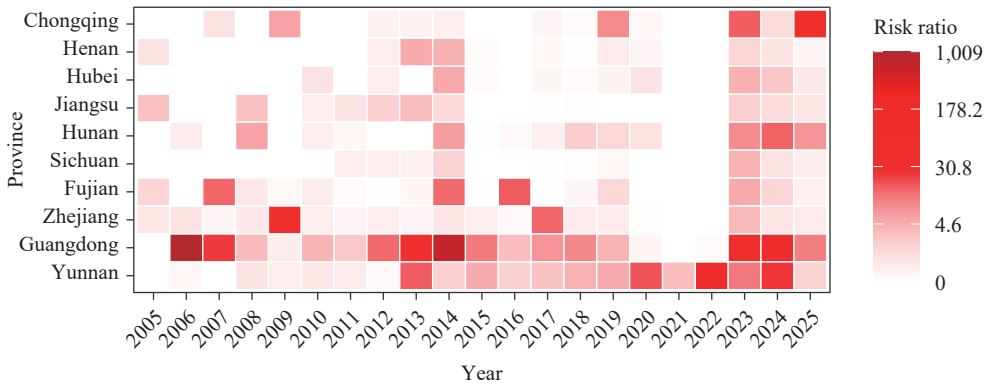

FIGURE 2. Transmission risk associated with imported dengue fever cases in the top 10 PLADs of China.
Abbreviation: PLAD=provincial-level administrative division.

and 2024 (81.1) (Figure 2). The sustained high ratios in these PLADs indicate a high potential for imported cases to trigger substantial local epidemics.

PLADs with intermittent high-risk outbreaks. Several PLADs experienced intermittent high-risk outbreaks. Zhejiang Province exhibited notable peaks in 2009 (39.8) and 2017 (15.2). Fujian Province recorded peaks in 2007 (14.9), 2011 (11.0), and 2016 (16.8). Hunan and Chongqing showed a sharp increase in risk in recent years, with Hunan's ratio rising to 15.5 in 2024 and 36.5 in 2025 (Figure 2). This pattern suggests sporadic, intense local transmission events following import.

PLADs with consistently low risk. Sichuan, Jiangsu, Hubei, and Henan provinces generally had low or very low risk ratios. In most years, ratios were at or near 0. Minor, sporadic increases occurred, such as in Hubei in 2014 (5.3) and 2023 (4.6) (Figure 2); however, these were limited in scale and duration. The epidemiology in these PLADs is characterized by imported cases with a low propensity to spark major local outbreaks.

Population Characteristics

From 2005 to 2025, males accounted for 53.7% of dengue fever cases in China. There was a significant gender disparity in the gender distribution between indigenous and imported cases (χ^2=2000.51, P<0.01) (Table 4). In terms of age distribution, indigenous dengue fever cases were older [40 (27, 55) years] than imported cases [36 (28, 45) years] (z=27.783, P<0.01). The 25–49 age group constituted the majority of cases, with a higher proportion of imported cases than indigenous cases. Conversely, individuals aged 70 years and above were more prevalent among indigenous cases (Table 4). Among indigenous cases, the highest proportion were unemployed individuals and retirees, whereas the most common occupations among imported cases were farmers and workers.

The distribution of indigenous and imported cases among different genders, age groups, and occupational populations in Guangdong exhibited significant differences (Table 4). 71.6% of indigenous cases were distributed in the 25–69 age group, with the highest proportion (35.7%) being unemployed household workers and retirees. The imported cases were predominantly male (25–49 years), mainly commercial and public place service personnel (30.2%), farmers and workers (25.5%), and unemployed household workers and retirees (23.9%). The differences in indigenous and imported cases among genders, age groups, and occupations in Yunnan were also statistically significant (Table 4). Occupational distribution was primarily farmers and workers (33.8%), unemployed household workers and retirees (20.2%), and commercial and public place service personnel (19.8%). The proportion of farmers and workers in imported cases (50.5%) was higher than among indigenous cases (31.4%).

DISCUSSION

This study analyzed the epidemiological characteristics of imported and indigenous dengue fever cases and dynamic provincial transmission risks in China from 2005 to 2025. The key findings and innovations are discussed below:

First, a key innovation of this study is the dynamic stratification and pattern identification of local transmission risk across ten key PLADs using the risk ratio metric. The results not only reaffirm the status of Yunnan and Guangdong as persistently high-risk PLADs (*8*–*9*) but also identify PLADs with intermittent high-risk outbreaks and those with consistently low risk. This approach moves beyond previous studies that primarily described absolute case numbers or spatial distribution (*10*–*11*), offering a quantitative framework to assess the efficiency or vulnerability of different PLADs in converting imported cases into local epidemics. Notably, the sharp increase in risk ratios in PLADs such as Hunan and Chongqing during 2023–2025 signals that these areas are emerging as high-risk frontiers, with critical implications for early warning and resource allocation.

Second, our study delineates the strong association between the seasonality of local transmission and the importation of cases. We found that indigenous cases were overwhelmingly concentrated from August to October, while imported cases began to increase significantly before the local epidemic season (e.g., May and June), confirming that imported cases serve as a crucial trigger for local outbreaks. This aligns with previous research that identified international travel as the primary pathway for viral introduction (*5*–*6*). However, by moving beyond the focus on import risk and air travel models from Southeast Asia (*5*), our study quantitatively assessed the spatiotemporal heterogeneity in the relative risk of local outbreaks following importation across different PLADs using a 21-year risk ratio. This represents a significant advancement in the understanding of varying provincial vulnerabilities to seeded outbreaks (*7*).

Third, our study systematically characterizes dynamic shifts in primary source countries and reveals distinct provincial importation profiles. Nationally, the dominant source country shifted from Cambodia (2015–2019) to Myanmar (2020–2025), reflecting changing epidemic landscapes in neighboring countries and the situation of personnel exchanges with China. More importantly, we identified fundamental differences between Yunnan and Guangdong provinces. Imported cases in Yunnan were highly concentrated from Myanmar and predominantly involved “farmers and workers,” highlighting a cross-border pattern of labor migration. In contrast, Guangdong received imported cases from more diverse sources, with “commercial/service personnel” being the largest occupational group. These findings extend the observations by Yue et al. (2021) on source countries for these two provinces (2004–2018) and provide more recent evidence of the shift toward Myanmar. They also reveal stark contrasts in the occupational structure of imported cases, offering precise demographic insights for targeted border surveillance (*8*).

Compared with previous national studies, our analysis covers the entire period before, during, and after the COVID-19 pandemic (*14*). The sharp decline

TABLE 4. Population characteristics of imported and indigenous dengue cases.

Region	Group		Total, *n* (%)	Indigenous cases, *n* (%)	Imported cases, *n* (%)	χ^2 value	*P*
Nationwide	Gender	Male	80,029 (53.7)	69,521 (51.8)	10,508 (71.2)	2,000.51	<0.01
		Female	68,864 (46.3)	64,608 (48.2)	4,256 (28.8)		
	Age group (years)	0–9	5,744 (3.9)	5,530 (4.1)	214 (1.5)	3,478.55	<0.01
		10–24	21,897 (14.7)	20,149 (15.0)	1,748 (11.8)		
		25–49	72,713 (48.8)	62,307 (46.5)	10,406 (70.5)		
		50–69	37,570 (25.2)	35,302 (26.3)	2,268 (15.4)		
		70+	10,969 (7.4)	10,841 (8.1)	128 (0.9)		
	Occupation	Household/unemployed/ retired persons	45,687 (30.7)	43,061 (32.1)	2,626 (17.8)	3,114.62	<0.01
		Farmers and workers	38,218 (25.7)	32,527 (24.2)	5,693 (38.6)		
		Commercial/service personnel	24,555 (16.5)	21,178 (15.8)	3,377 (22.9)		
		Teachers and students	16,369 (11.0)	15,490 (11.5)	879 (6.0)		
		Other occupations and unknown	14,285 (9.6)	13,310 (9.9)	975 (6.6)		
		Staff members	6,114 (4.1)	5,172 (3.9)	942 (6.4)		
		Individuals and freelancers	3,663 (2.5)	3,391 (2.5)	272 (1.8)		
Guangdong	Gender	Male	46,808 (52.3)	44,707 (51.6)	2,101 (71.0)	428.30	<0.01
		Female	42,718 (47.7)	41,859 (48.4)	859 (29.0)		
	Age group (years)	0–9	3,626 (4.1)	3,609 (4.2)	17 (0.6)	975.71	<0.01
		10–24	13,893 (15.5)	13,537 (15.6)	356 (12.0)		
		25–49	42,836 (47.3)	40,192 (46.4)	2,194 (74.1)		
		50–69	22,214 (24.8)	21,841 (25.2)	373 (12.6)		
		70+	7,407 (8.3)	7,387 (8.5)	20 (0.7)		
	Occupation	Household/unemployed/ retired persons	31,992 (35.7)	31,284 (36.1)	708 (23.9)	887.50	<0.01
		Farmers and workers	18,153 (20.3)	17,398 (20.1)	755 (25.5)		
		Commercial/service personnel	14,027 (15.7)	13,134 (15.2)	893 (30.2)		
		Other occupations and unknown	10,810 (12.1)	10,605 (12.3)	205 (6.9)		
		Teachers and students	10,160 (11.3)	10,025 (11.6)	135 (4.6)		
		Staff members	3,260 (3.6)	3,038 (3.5)	222 (7.5)		
		Individuals and freelancers	1,124 (1.3)	1,082 (1.2)	42 (1.4)		
Yunnan	Gender	Male	18,026 (54.7)	15,327 (53.3)	2,699 (64.7)	191.33	<0.01
		Female	14,918 (45.3)	13,444 (46.7)	1,474 (35.3)		
	Age group (years)	0–9	1,438 (4.4)	1,297 (4.5)	141 (3.4)	449.01	<0.01
		10–24	4,822 (14.6)	4,238 (14.7)	584 (14.0)		
		25–49	16,591 (50.4)	13,920 (48.4)	2,671 (64.0)		
		50–69	8,207 (24.9)	7,498 (26.1)	709 (17.0)		
		70+	1,886 (5.7)	1818 (6.3)	68 (1.6)		
	Occupation	Farmers and workers	11,149 (33.8)	9,040 (31.4)	2,109 (50.5)	946.76	<0.01
		Household/unemployed/ retired persons	6,647 (20.2)	6,298 (21.9)	349 (8.4)		
		Commercial/service personnel	6,518 (19.8)	5523 (19.2)	995 (23.8)		
		Teachers and students	3,510 (10.7)	3,172 (11.0)	338 (8.1)		
		Individuals and freelancers	2,073 (6.3)	1,972 (6.9)	101 (2.4)		
		Other occupations and unknown	1,852 (5.6)	1,705 (5.9)	147 (3.5)		
		Staff members	1,195 (3.6)	1,061 (3.7)	134 (3.2)		

in indigenous cases in 2020–2021 due to non-pharmaceutical interventions (NPIs), followed by a rapid rebound of both imported and indigenous cases post-2022, reaching a historical sub-peak in 2024, corroborates the complex impact of NPIs on dengue transmission, as reviewed by Wu et al. (2022), and provides the latest empirical evidence from China (*15*).

This study has several limitations. First, under-reporting of surveillance data, particularly for mild and asymptomatic infections, is a possibility (*16*). In addition, disparities in monitoring capabilities across PLADs may have led to data bias. Second, the study primarily analyzed dengue fever-reported cases in Chinese mainland, excluding cases from Hong Kong Special Administrative Region (SAR), Macao SAR, and Taiwan, China; therefore, the analysis of importation risk may be incomplete. Moreover, this study did not control for confounding factors such as temperature, precipitation, and mosquito vector density when analyzing case counts. The hazard ratio was calculated from the reported case numbers, without accounting for potential confounding factors. Future research could integrate multisource data to build more refined risk-prediction models.

In summary, this study underscores the limitations of a "one-size-fits-all" control strategy. Future prevention and control efforts should transition toward precision strategies based on provincial risk profiles. These strategies include enhanced monitoring and health education for travelers from specific source countries (e.g., Myanmar) and occupational groups (e.g., laborers) in border PLADs such as Yunnan; strengthened screening of travelers from multiple endemic areas in commercial hubs such as Guangdong; and preemptive reinforcement of vector surveillance and response capacity in emerging high-risk PLADs such as Hunan and Chongqing. Continuous monitoring of dynamic changes in importation sources remains vital.

Conflicts of interest: No conflicts of interest.

Funding: Supported by the National Major Science and Technology Project on Emerging and Outbreak Infectious Diseases Prevention and Control (2026ZD01908803).

doi: 10.46234/ccdcw2026.089

[#] Corresponding author: Qiulan Chen, chenql@chinacdc.cn.

[1] National Key Laboratory of Intelligent Tracking and Forecasting for Infectious Diseases, Division of Infectious Dieases, Branch of Vector-borne Diseases, Chinese Center for Disease Control and Prevention & Chinese Academy of Preventive Medicine, Beijing, China; [2] School of Public Health, Guangxi Medical University, Nanning City, Guangxi Zhuang Autonomous Region, China.

Submitted: January 30, 2026
Accepted: April 25, 2026
Issued: May 01, 2026

REFERENCES

1. Yang XR, Quam MBM, Zhang TC, Sang SW. Global burden for dengue and the evolving pattern in the past 30 years. J Travel Med 2021;28(8):taab146. https://doi.org/10.1093/jtm/taab146.
2. Wilder-Smith A, Ooi EE, Horstick O, Wills B. Dengue. Lancet 2019;393(10169):350 – 63. https://doi.org/10.1016/S0140-6736(18)32560-1.
3. WHO. Global dengue surveillance. [2026-01-30]. https://worldhealthorg.shinyapps.io/dengue_global/.
4. Tsheten T, Gray DJ, Clements ACA, Wangdi K. Epidemiology and challenges of dengue surveillance in the WHO South-East Asia Region. Trans R Soc Trop Med Hyg 2021;115(6):583 – 99. https://doi.org/10.1093/trstmh/traa158.
5. Lai SJ, Johansson MA, Yin WW, Wardrop NA, Van Panhuis WG, Wesolowski A, et al. Seasonal and interannual risks of dengue introduction from South-East Asia into China, 2005-2015. PLoS Negl Trop Dis 2018;12(11):e0006743. https://doi.org/10.1371/journal.pntd.0006743.
6. Lun X, Wang YG, Zhao CC, Wu HX, Zhu CY, Ma DL, et al. Epidemiological characteristics and temporal-spatial analysis of overseas imported dengue fever cases in outbreak provinces of China, 2005–2019. Infect Dis Poverty 2022;11(1):12. https://doi.org/10.1186/s40249-022-00937-5.
7. Zhai HR, Qin HJ, Chen JY, Ren Q, Mu D, Chen QL, et al. Changing epidemiologic characteristics of dengue fever in Chinese mainland between 2019 and 2024. Zoonoses 2025;5(1):961. https://doi.org/10.15212/zoonoses-2024-0069.
8. Yue YJ, Liu QY, Liu XB, Wu HX, Xu MF. Comparative analyses on epidemiological characteristics of dengue fever in Guangdong and Yunnan, China, 2004-2018. BMC Public Health 2021;21(1):1389. https://doi.org/10.1186/s12889-021-11323-5.
9. Deng SZ, Liu XY, Su JJ, Xiang LH, Chang LT, Zhu JJ, et al. Epidemiological and cluster characteristics of dengue fever in Yunnan Province, Southwestern China, 2013-2023. BMC Infect Dis 2025;25(1):95. https://doi.org/10.1186/s12879-024-10403-2.
10. Yue YJ, Liu XB, Ren DS, Wu HX, Liu QY. Spatial dynamics of dengue fever in mainland China, 2019. Int J Environ Res Public Health 2021;18(6):2855. https://doi.org/10.3390/ijerph18062855.
11. Ni HB, Cai XY, Ren JR, Dai TT, Zhou JY, Lin JM, et al. Epidemiological characteristics and transmission dynamics of dengue fever in China. Nat Commun 2024;15(1):8060. https://doi.org/10.1038/s41467-024-52460-w.
12. National Health and Family Planning Commission of the People's Republic of China. WS 216-2018 Diagnosis for dengue fever. Beijing: China Standards Press, 2018. http://www.csres.com/detail/312267.html. (In Chinese).
13. National Disease Control and Prevention Administration. Technical Guidelines for Dengue Fever Prevention and Control (2025 Edition) [J]. *Chinese Journal of Virology* 2025, 15(05): 417-425.(In Chinese).
14. Yue YJ, Liu XB, Ren DS, Yin WW. Epidemiological characteristics of dengue fever in Chinese Mainland, 2005-2020. Chin J Vector Biol Control 2023;34(6):761 – 6,818. https://doi.org/10.11853/j.issn.1003.8280.2023.06.010.
15. Wu Q, Dong SW, Li XK, Yi BY, Hu H, Guo ZM, et al. Effects of COVID-19 non-pharmacological interventions on dengue infection: a systematic review and meta-analysis. Front Cell Infect Microbiol 2022;12:892508. https://doi.org/10.3389/fcimb.2022.892508.
16. World Health Organization. Report on the global arbovirus surveillance and response capacity survey 2021-2022. [2026-01-30]. https://www.who.int/ publications/b/77071.

SUPPLEMENTARY MATERIAL

SUPPLEMENTARY TABLE S1. Cumulative monthly distribution of imported and indigenous cases, 2005–2025.

Month	Total, *n* (%)	Imported cases (%)	Indigenous cases (%)
January	428 (100.0)	414 (96.7)	14 (3.3)
February	320 (100.0)	306 (95.6)	14 (4.4)
March	274 (100.0)	264 (96.4)	10 (3.6)
April	479 (100.0)	455 (95.0)	24 (5.0)
May	917 (100.0)	848 (92.5)	69 (7.5)
June	1,764 (100.0)	1,433 (81.2)	331 (18.8)
July	5,630 (100.0)	1,907 (33.9)	3,723 (66.1)
August	18,416 (100.0)	2,423 (13.2)	15,993 (86.8)
September	50,378 (100.0)	2,452 (4.9)	47,926 (95.1)
October	57,191 (100.0)	2,225 (3.9)	54,966 (96.1)
November	11,999 (100.0)	1,409 (11.7)	10,590 (88.3)
December	1,097 (100.0)	628 (57.2)	469 (42.8)
Total	148,893 (100.0)	14,764 (9.9)	134,129 (90.1)

SUPPLEMENTARY TABLE S2. Cumulative number of imported and indigenous cases of dengue by region across China, 2005–2025.

PLADs	Total, *n* (%)	Indigenous cases (%)	Imported cases (%)	PLADs	Total, *n* (%)	Indigenous cases (%)	Imported cases (%)
Guangdong	89,526 (100.0)	86,566 (96.7)	2,960 (3.3)	Beijing	256 (100.0)	44 (17.2)	212 (82.8)
Yunnan	32,944 (100.0)	28,771 (87.3)	4,173 (12.7)	Guizhou	167 (100.0)	78 (46.7)	89 (53.3)
Guangxi	4,398 (100.0)	4,179 (95.0)	219 (5.0)	Hebei	157 (100.0)	27 (17.2)	130 (82.8)
Fujian	4,041 (100.0)	2,683 (66.4)	1,358 (33.6)	Shaanxi	123 (100.0)	33 (26.8)	90 (73.2)
Zhejiang	3,797 (100.0)	2,402 (63.3)	1,395 (36.7)	Liaoning	116 (100.0)	32 (27.6)	84 (72.4)
Chongqing	3,723 (100.0)	3,402 (91.4)	321 (8.6)	Heilongjiang	43 (100.0)	9 (20.9)	34 (79.1)
Hunan	2,879 (100.0)	2,276 (79.1)	603 (20.9)	Gansu	33 (100.0)	9 (27.3)	24 (72.7)
Jiangxi	1,598 (100.0)	1,346 (84.2)	252 (15.8)	Shanxi	33 (100.0)	11 (33.3)	22 (66.7)
Hainan	977 (100.0)	865 (88.5)	112 (11.5)	Tianjin	33 (100.0)	3 (9.1)	30 (90.9)
Sichuan	976 (100.0)	342 (35.0)	633 (65.0)	Jilin	25 (100.0)	3 (12.0)	22 (88.0)
Jiangsu	734 (100.0)	233 (31.7)	501 (68.3)	Inner Mongolia	15 (100.0)	6 (40.0)	9 (60.0)
Hubei	715 (100.0)	324 (45.3)	391 (54.7)	Ningxia	11 (100.0)	0 (0.0)	11 (100.0)
Henan	627 (100.0)	243 (38.8)	384 (61.2)	Xinjiang	9 (100.0)	5 (55.6)	4 (44.4)
Shandong	365 (100.0)	108 (29.6)	257 (70.4)	Qinghai	4 (100.0)	3 (75.0)	1 (25.0)
Shanghai	310 (100.0)	74 (23.9)	236 (76.1)	Xizang	1 (100.0)	0 (0.0)	1 (100.0)
Anhui	257 (100.0)	52 (20.2)	205 (79.8)	Total	148,893 (100.0)	134,129 (90.1)	14,764 (9.9)

Abbreviation: PLAD=provincial-level administrative division.

Preplanned Studies

A Topographic Analysis of Malaria Transmission — Khyber Pakhtunkhwa, Pakistan, 2019–2022

Ijaz ul Haq[1,#]

Summary

What is already known about this topic?

Malaria remains a recurrent public health problem and is among the leading contributors to morbidity and mortality in Pakistan. However, research specifically linking malaria transmission with topographic factors in Pakistan is limited.

What is added by this report?

This study supplements existing knowledge by examining malaria transmission across different topographic regions of Khyber Pakhtunkhwa Province, Pakistan. High-altitude regions experienced low transmission, whereas low-altitude regions showed high transmission rates.

What are the implications for public health practice?

Considering topography in malaria control strategies may help policymakers design more targeted and effective prevention measures to reduce the burden of recurrent malaria in the region.

ABSTRACT

Introduction: Malaria is a major public health concern in Pakistan. Data examining the relation between topography and malaria transmission in Pakistan are limited. This study aimed to analyze malaria transmission in relation to topography across Khyber Pakhtunkhwa from 2019 to 2022.

Methods: This retrospective study analyzed malaria case data collected from the provincial health department, the District Health Information System, and district health offices across Khyber Pakhtunkhwa. Time-series analysis was conducted to determine malaria trends over time.

Results: The results showed the highest cumulative case counts in Charsadda (303,900), Dera Ismail Khan (292,070), and Bannu (241,640), whereas high-altitude districts, such as Kolai Palas (2.56 km), reported far fewer cases (<1,000). These findings indicate an inverse relation between altitude and malaria incidence, highlighting high vector density in low-altitude regions.

Conclusion: Topography strongly influences malaria risk. Integrating elevation-based spatial data into provincial malaria control policies is recommended.

Malaria remains a major public health concern, with more than 282 million cases and over 610,000 deaths reported worldwide by 2024, despite decades of progress in control and prevention efforts. Millions of people in Pakistan are affected annually (*1*). The global disease burden of malaria is particularly high in sub-Saharan Africa and parts of Asia, where environmental and geographical conditions strongly influence the transmission dynamics of *Plasmodium* parasites (*2*). Malaria control strategies in Pakistan focus on optimal resource allocation to enhance surveillance and reduce disease burden, particularly in the context of population vulnerability, displacement, and climate change (*3*).

Despite intensive efforts to eliminate malaria since the 1960s, the disease resurged in the 1970s and has remained endemic in several regions because of multiple factors, including environmental and socioeconomic conditions that contribute to transmission (*4*). Topography is an important determinant of malaria transmission, as regions with high elevation and low temperatures generally exhibit low transmission risk (*5*). However, recent advances in spatial modeling, remote sensing, and Geographic Information Systems have enhanced malaria risk assessment by producing high-resolution risk maps (*6*).

Malaria is recurrent across all provinces of Pakistan; however, the country remains a low-resource setting and bears a high burden of malaria-related morbidity, mortality, and prevention costs. Topographic variations in Khyber Pakhtunkhwa (KP) have not been adequately considered in previous analyses. Therefore, this study analyzed malaria transmission patterns in KP

from 2019 to 2022.

Secondary data on malaria incidence were obtained from the Provincial District Health Information System and District Health Offices across multiple districts. These data included the number of malaria cases reported in each district. Case records were initially verified by a district medical entomologist and subsequently approved by a provincial medical entomologist. Blood smear microscopy was used for malaria diagnosis (*1*). Data on latitude, longitude, and altitude were obtained from the Provincial Meteorological Department, Peshawar.

KP is located in northwestern Pakistan and is the third most populous province in the country. The study population included all districts of KP, while the target population comprised malaria-sensitive districts. The province was categorized into three zones to assess the impact of topography on malaria transmission:

Southern KP: Bannu, Tank, Karak, and Dera Ismail Khan.

Northern KP: Haripur, Abbottabad, Dir, Kohistan, Swat, and Chitral.

Central KP: Peshawar, Charsadda, Nowshera, and Mardan.

Districts were further classified as low-altitude (<0.46 km), mid-altitude (0.46–1.22 km), and high-altitude (>1.22 km; Supplementary Table S1, available at https://weekly.chinacdc.cn/).

The topographic distribution of KP highlighting high-altitude regions, such as Chitral and Swat, and low-altitude regions, such as Bannu and Dera Ismail Khan.

Statistical analyses were performed using SPSS (version 25.0, Armonk, NY, USA: IBM Corp.). Pearson's correlation analysis was used to assess the association between altitude and malaria incidence. QGIS software was used to generate maps and figures. A time-series analysis was conducted to examine malaria trends across KP districts. Space–time permutation scan statistics were applied to identify malaria hotspots in the region.

The incidence of malaria varies across the topography of KP from 2019 to 2022. Between 2019 and 2022, the confirmed malaria cases varied significantly across the KP districts (Table 1). Charsadda had the highest cumulative burden (303,900 cases), followed by Dera Ismail Khan (292,070 cases), Bannu (241,640 cases), and Mardan (233,749 cases). By contrast, districts, such as Kohistan Lower (423 cases), Kolai Palas (606 cases), and Kohistan Upper (1,637 cases), recorded the lowest number of cases. Districts with low altitudes, such as Dera Ismail Khan (0.18 km) and Lakki Marwat (0.17 km), reported high case numbers, whereas high-altitude regions, such as Kolai Palas (2.56 km) and Kohistan Upper (1.91 km), showed markedly fewer cases. Malaria incidence per 10,000 population is shown in Supplementary Table S1, which indicates that northern districts have a lower incidence than southern districts with low altitude.

Districts, such as Bannu, Dera Ismail Khan, and Lakki Marwat, are located at low altitude but accounted for more than 60% of cases; similarly, in central KP, Peshawar, Mardan, Charsadda, and Nowshera recorded higher confirmed malaria cases compared with those of other districts of KP (Figure 1). A negative correlation was observed between altitude and malaria incidence rates from 2019 to 2022 (Figure 2). Space–time permutation analysis was used to identify hotspot districts based on incidence (Supplementary Figure S1, available at https://weekly.chinacdc.cn/). Lakki Marwat and Tank, located at low altitudes, exhibited the highest incidence rates, indicating persistent spatial hotspots, whereas Shangla, Hangu, and Bannu demonstrated emerging and expanding temporal risks. Districts located at low altitudes (<1,500 ft) had a high malaria burden, whereas high-altitude districts (>4,000 ft) consistently reported low case counts.

DISCUSSION

This study investigated the spatial distribution of malaria incidence based on topographic features across several districts of KP, Pakistan. The findings demonstrate a strong association between malaria incidence and topographic factors.

Spatial heterogeneity in vector density and disease risk has emerged as a major concern. Kouame et al. showed that even within the same region, the relation between vector abundance and malaria incidence may differ because of local geographical and environmental factors (*7*). This insight is particularly important in the context of KP, where variable topography creates localized transmission patterns that cannot be addressed using uniform control approaches. In our study, malaria incidence hotspot districts were identified, showing that low-altitude areas had high malaria case counts. This pattern suggests that altitude plays a modifying role in malaria transmission within provinces. There is evidence that malaria transmission declines with increasing altitude, as highland areas

TABLE 1. District-wise confirmed malaria cases in Khyber Pakhtunkhwa.

District	2019 (*n*)	2020 (*n*)	2021 (*n*)	2022 (*n*)	Latitude (º N)	Longitude (º E)	Altitude (km)
Bannu	32,640	68,284	70,983	69,733	32.986	70.604	0.36*
Dera Ismail Khan	51,209	78,252	75,800	86,809	31.862	70.901	0.18*
Lakki Marwat	34,240	50,705	48,114	85,480	32.613	70.901	0.17*
Tank	25,734	22,807	25,132	33,576	32.216	70.389	0.26*
Abbottabad	1,861	190	923	474	34.168	73.221	1.26§
Haripur	7,263	3,530	3,996	5,019	33.994	72.910	0.52†
Kohistan Upper	402	133	412	690	34.250	73.500	1.91§
Mansehra	1,901	1,087	1,586	1,756	34.331	73.198	1.09†
Battagram	419	632	279	2,352	34.672	73.024	1.04†
Tor Ghar	1,821	525	266	1,907	34.449	70.199	2.44§
Kohistan Lower	20	62	169	172	35.250	73.500	1.68§
Kolai-Palas	20	24	100	462	35.100	73.000	2.56§
Karak	13,243	17,306	17,084	25,813	33.111	71.091	0.55†
Kohat	22,048	24,612	25,746	40,640	33.589	71.443	0.49†
Hangu	13,073	17,598	21,335	31,138	33.522	71.062	0.81†
Buner	21,096	18,184	32,177	48,014	34.394	72.615	0.80†
Chitral Lower	6,621	3,327	5,445	4,143	35.370	71.740	1.49§
Dir Lower	27,721	27,640	39,994	47,309	35.370	71.740	0.97†
Malakand	16,711	11,886	14,543	20,104	34.503	71.905	0.45*
Swat	21,085	23,280	17,684	14,066	35.223	72.426	0.98†
Dir Upper	12,883	11,434	12,011	7,234	35.208	71.875	1.84§
Shangla	14,419	20,157	26,066	41,316	34.802	72.757	1.52§
Chitral Upper	679	332	484	453	35.833	71.783	1.50§
Mardan	45,446	48,968	57,322	82,013	34.199	72.040	0.28*
Swabi	7,182	4,589	4,527	4,230	34.117	72.281	0.34*
Charsadda	53,718	74,692	87,219	88,271	34.149	71.743	0.30*
Nowshera	29,467	20,780	29,518	43,286	34.011	71.988	0.55†
Peshawar	8,852	7,274	10,713	37,370	34.026	71.560	0.37*

* means low altitude (<0.46 km);
† means mid-altitude (0.46–1.22 km);
§ means high altitude (>1.22 km).

report significantly fewer cases than those of low-altitude areas (*8*). Previous studies have developed high-resolution malaria models incorporating population density, climate, and surface hydrology (*9*). In our study, districts with seasonal flooding and irrigation infrastructure had high malaria incidence, which is consistent with these findings. Furthermore, our results align with those of studies from Africa that identified significant associations between malaria frequency and topographic variables, such as elevation and slope. Their spatial modeling approaches informed the analytical framework of our study, underscoring the need to incorporate topography into disease surveillance systems. High topographic features restrict malaria transmission from highland areas to lowlands, where malaria-related morbidity is high (*2*).

Geographical highlands influence vector density. Bannu District, a southern district, has a low altitude but high mosquito density, which leads to elevated malaria prevalence. Malaria transmission is higher in KP than in other provinces, such as Punjab and Sindh (*3*). Punjab may have more effective vector control strategies. In addition to altitude, increased temperature (≥22.4 °C) enhances vector density and, consequently, malaria transmission (*10*). Climatic factors, such as high rainfall, humidity, and flooding, promote habitat development, vector population growth, vector longevity, and breeding site availability,

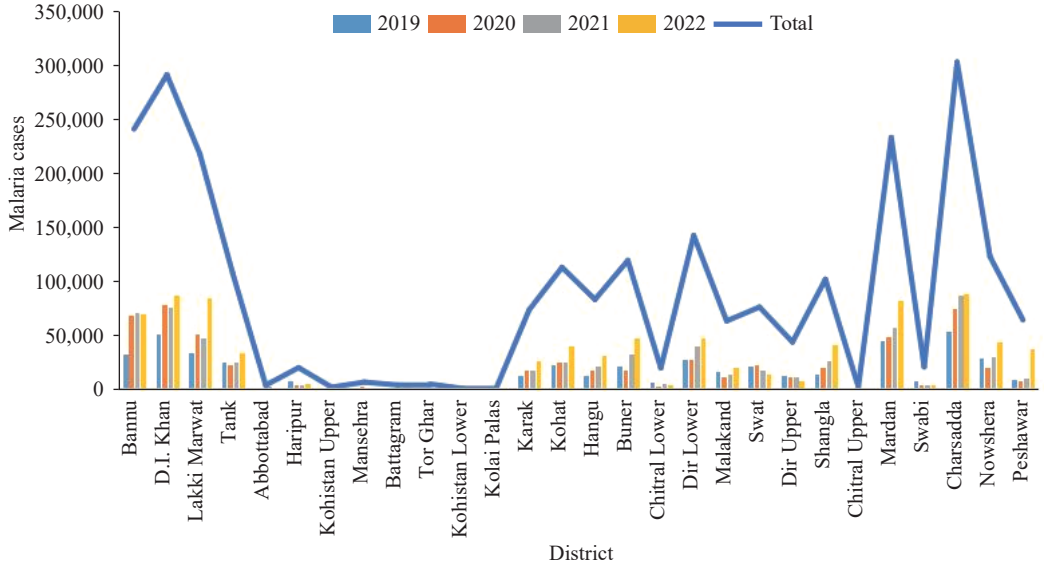

FIGURE 1. Confirmed malaria cases in various districts of Khyber Pakhtunkhwa, Pakistan.
Note: Low-altitude districts [including Bannu and Dera Ismail (D.I) Khan] accounted for more than 60% of total cases.

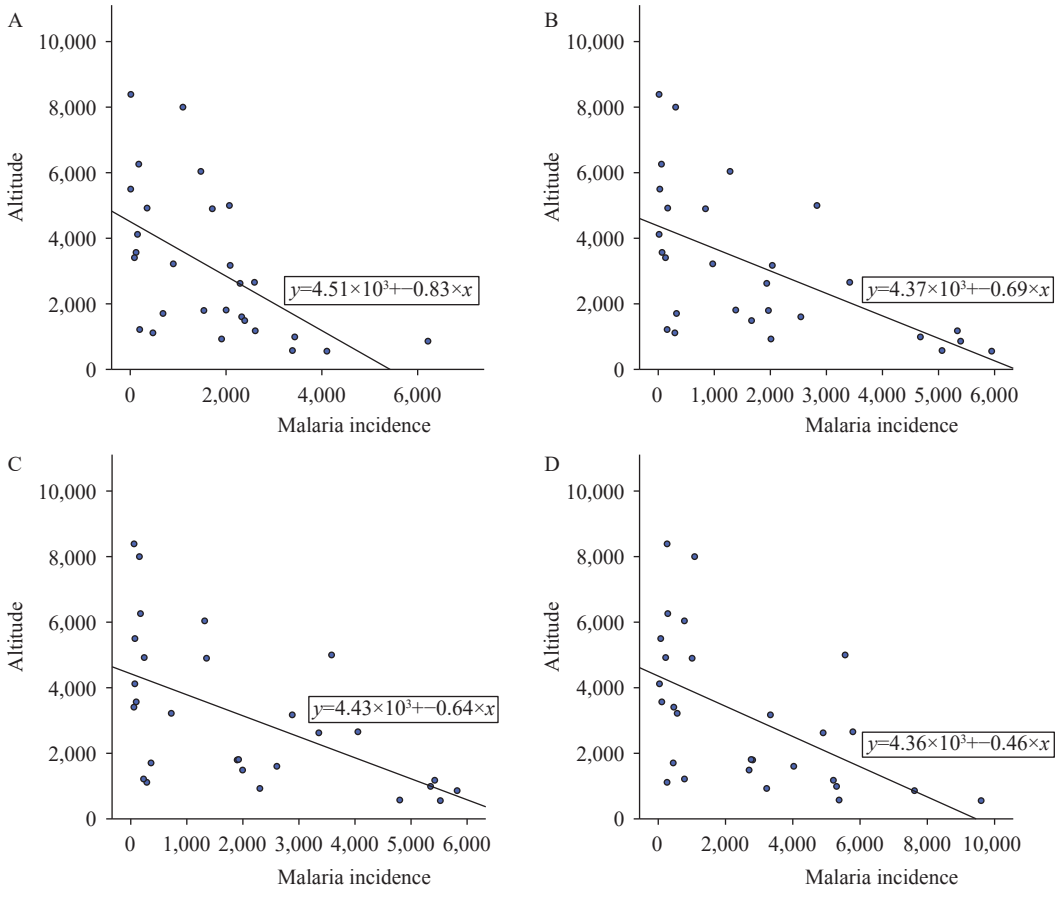

FIGURE 2. Scatter plot of altitude versus malaria incidence rates in Khyber Pakhtunkhwa. (A) 2019; (B) 2020; (C) 2021; (D) 2022.
Note: There was a negative correlation between altitude and malaria incidence across the study period; the altitude was measured in feet.

thereby facilitating malaria transmission. Several studies have examined malaria incidence in parts of KP; however, these efforts have largely been limited to district-level analyses or have focused primarily on environmental factors (*3*,*10*). These studies assessed the effects of temperature, humidity, and rainfall on malaria incidence in Pakistan. By contrast, there remains a lack of systematic topographic evaluations assessing how elevation, slope, and terrain influence malaria transmission across Pakistan, particularly in KP. Furthermore, no previous study has specifically examined spatial trends using province-wide data from KP.

This study has some limitations. First, data were obtained from the District Health Information System and district health offices. Malaria cases are often underreported because of poor communication or because hospital and facility staff are engaged in competing responsibilities. Second, at the district level, there is typically only one medical epidemiologist responsible for multiple facilities, which further contributes to data limitations.

In conclusion, this study highlighted the importance of topography in malaria transmission. High altitudes were associated with few cases, whereas low altitudes were associated with high malaria transmission in KP. Altitude was negatively correlated with malaria incidence throughout the study period. Low-altitude districts with a high malaria burden require weekly surveillance, including hotspot mapping and the allocation of up to 150,000 rapid diagnostic tests (RDTs) per year. Mid-altitude districts require biweekly monitoring, hotspot mapping, and the allocation of up to 70,000 RDTs per year. High-altitude districts with a low malaria burden require monthly surveillance, hotspot monitoring, and the allocation of up to 10,000 RDTs per year. Policymakers should consider altitude-related risks in hotspot areas when designing malaria prevention strategies in the region.

Conflicts of interest: No conflict of interest.

Acknowledgements: The Deanship for Scientific Research, King Faisal University, Saudi Arabia, for funding this study.

Ethical statement: Ethical approval for this study was obtained from the Ethics Review Board of the University of Agriculture, Pakistan.

Funding: Funding Statement: Supported by the Deanship for Scientific Research, King Faisal University, Saudi Arabia (grant number KFU260322).

doi: 10.46234/ccdcw2026.090

[#] Corresponding author: Ijaz ul Haq, ihaq@kfu.edu.sa.

[1] Department of Clinical Nutrition, College of Applied Medical Sciences, King Faisal University, Al Hofuf, Al-Ahsa, Saudi Arabia.

Submitted: September 04, 2025
Accepted: February 14, 2026
Issued: May 01, 2026

REFERENCES

1. WHO. World malaria report 2025. 2025. https://www.who.int/teams/global-malaria-programme/reports/world-malaria-report-2025. [2025-9-3].
2. Atieli HE, Zhou GF, Lee MC, Kweka EJ, Afrane Y, Mwanzo I, et al. Topography as a modifier of breeding habitats and concurrent vulnerability to malaria risk in the western Kenya highlands. Parasit Vectors 2011;4(1):241. https://doi.org/10.1186/1756-3305-4-241.
3. Haq IU, Mehmood Z, Khan GA, Kainat B, Ahmed B, Shah J, et al. Modeling the effect of climatic conditions and topography on malaria incidence using Poisson regression: a Retrospective study in Bannu, Khyber Pakhtunkhwa, Pakistan. Front Microbiol 2024;14:1303087. https://doi.org/10.3389/fmicb.2023.1303087.
4. Umer MF, Zofeen S, Majeed A, Hu WB, Qi X, Zhuang GH. Effects of socio-environmental factors on malaria infection in Pakistan: a Bayesian spatial analysis. Int J Environ Res Public Health 2019;16(8):1365. https://doi.org/10.3390/ijerph16081365.
5. Dabaro D, Birhanu Z, Negash A, Hawaria D, Yewhalaw D. Effects of rainfall, temperature and topography on malaria incidence in elimination targeted district of Ethiopia. Malar J 2021;20(1):104. https://doi.org/10.1186/s12936-021-03641-1.
6. Hay SI, Snow RW. The malaria Atlas Project: developing global maps of malaria risk. PLoS Med 2006;3(12):e473. https://doi.org/10.1371/journal.pmed.0030473.
7. Kouame RMA, Edi AVC, Cain RJ, Weetman D, Donnelly MJ, Sedda L. Joint spatial modelling of malaria incidence and vector's abundance shows heterogeneity in malaria-vector geographical relationships. J Appl Ecol 2024;61(2):365 – 78. https://doi.org/10.1111/1365-2664.14565.
8. Bødker R, Akida J, Shayo D, Kisinza W, Msangeni HA, Pedersen EM, et al. Relationship between altitude and intensity of malaria transmission in the Usambara Mountains, Tanzania. J Med Entomol 2003;40(5):706 – 17. https://doi.org/10.1603/0022-2585-40.5.706.
9. Tompkins AM, Ermert V. A regional-scale, high resolution dynamical malaria model that accounts for population density, climate and surface hydrology. Malar J 2013;12(1):65. https://doi.org/10.1186/1475-2875-12-65.
10. Fatima SH, Zaidi F, Rafiq J, Bhandari D, Ali A, Bi P. Impact of temperatures on malaria incidence in vulnerable regions of Pakistan: empirical evidence and future projections. Epidemiol Infect 2025;153:e33. https://doi.org/10.1017/S0950268825000111.

SUPPLEMENTARY MATERIAL

SUPPLEMENTARY TABLE S1. Estimated district-wise population and malaria incidence per 100,000 population with 95% *CI* (2019–2022).

District	Pop.				Cases				Incidence/100,000*			
	2019	2020	2021	2022	2019	2020	2021	2022	2019	2020	2021	2022
Bannu	1,250,886	1,279,657	1,309,089	1,339,198	32,640	68,284	70,983	69,733	2,609.35 (2,575.28, 2,643.42)	5,336.12 (5,281.09, 5,391.16)	5,422.32 (5,365.58, 5,479.06)	5,207.07 (5,152.03, 5,262.11)
Dera Ismail Khan	1,512,447	1,545,721	1,579,727	1,614,481	51,209	78,252	75,800	86,809	3,385.84 (3,348.83, 3,422.85)	5,062.49 (5,011.44, 5,113.54)	4,798.30 (4,746.14, 4,850.46)	5,376.90 (5,323.48, 5,430.31)
Lakki Marwat	834,137	852,488	871,243	890,410	34,240	50,705	48,114	85,480	4,104.84 (4,044.34, 4,165.34)	5,947.88 (5,871.53, 6,024.23)	5,522.45 (5,448.25, 5,596.65)	9,600.07 (9,507.64, 9,692.50)
Tank	414,104	422,800	431,679	440,744	25,734	22,807	25,132	33,576	6,214.38 (6134.55, 6294.21)	5,394.28 (5325.83, 5462.73)	5,821.92 (5746.74, 5897.10)	7,618.03 (7528.20, 7707.86)
Abbottabad	1,228,714	1,253,288	1,278,354	1,303,921	1,861	190	923	474	151.46 (144.61, 158.31)	15.16 (8.67, 21.64)	72.20 (67.21, 77.19)	36.35 (33.09, 39.61)
Haripur	1,062,422	1,083,670	1,105,344	1,127,450	7,263	3,530	3,996	5,019	683.63 (668.84, 698.42)	325.74 (314.61, 336.87)	361.52 (349.72, 373.32)	445.16 (431.92, 458.40)
Kohistan Upper	226,487	232,149	237,953	243,902	402	133	412	690	177.49 (160.41, 194.57)	57.29 (48.00, 66.58)	173.14 (156.06, 190.22)	282.90 (262.52, 303.28)
Mansehra	1,564,393	1,597,245	1,630,787	1,665,034	1,901	1,087	1,586	1,756	121.52 (115.95, 127.09)	68.05 (63.81, 72.29)	97.25 (91.61, 102.89)	105.46 (99.82, 111.10)
Battagram	478,520	488,569	498,829	509,304	419	632	279	2,352	87.56 (79.44, 95.68)	129.36 (118.84, 139.88)	55.93 (49.36, 62.50)	461.81 (443.58, 480.04)
Tor Ghar	165,641	169,120	172,671	176,297	1,821	525	266	1,907	1,099.37 (1,047.35, 1,151.39)	310.43 (284.34, 336.52)	154.05 (137.86, 170.24)	1,081.70 (1,030.66, 1,132.74)
Kohistan Lower	217,428	222,863	228,435	234,146	20	62	169	172	9.20 (5.35, 13.05)	27.82 (21.04, 34.60)	73.98 (62.76, 85.20)	73.46 (62.23, 84.69)
Kolai-Palas	163,071	167,147	171,326	175,609	20	24	100	462	12.26 (7.09, 17.43)	14.36 (8.56, 20.16)	58.37 (47.60, 69.14)	263.08 (239.68, 286.48)
Karak	861,636	880,592	899,965	919,765	13,243	17,306	17,084	25,813	1,536.96 (1,509.83, 1,564.09)	1,965.27 (1,931.57, 1,998.97)	1,898.30 (1,865.07, 1,931.53)	2,806.48 (2,764.51, 2,848.45)
Kohat	947,838	967,742	988,065	100,8814	22,048	24,612	25,746	40,640	2,326.14 (2,291.65, 2,360.63)	2,543.24 (2,505.27, 2,581.21)	2,605.70 (2,567.05, 2,644.35)	4,028.49 (3,977.21, 4,079.77)
Hangu	504,149	515,240	526,575	538,160	13,073	17,598	21,335	31,138	2,593.08 (2,552.10, 2,634.06)	3,415.50 (3,360.11, 3,470.89)	4,051.65 (3,987.36, 4,115.94)	5,786.01 (5,712.45, 5,859.57)
Buner	920,231	939,556	959,286	979,431	2,1096	18,184	32,177	48,014	2,292.47 (2,248.01, 2,336.93)	1,935.38 (1,891.49, 1,979.27)	3,354.27 (3,297.77, 3,410.77)	4,902.23 (4,832.93, 4,971.53)
Chitral Lower	386,497	394,613	402,900	411,361	6,621	3,327	5,445	4,143	1,713.08 (1,669.04, 1,757.12)	843.10 (816.18, 870.02)	1,351.45 (1,307.02, 1,395.88)	1,007.14 (970.85, 1,043.43)
Dir Lower	1,329,120	1,358,361	1,388,245	1,418,786	27,721	27,640	39,994	47,309	2,085.67 (2,044.16, 2,127.18)	2,034.81 (1,993.22, 2,076.40)	2,880.90 (2,825.12, 2,936.68)	3,334.47 (3,274.19, 3,394.75)
Malakand	699,375	714,062	729,058	744,368	16,711	11,886	14,543	20,104	2,389.42 (2,343.19, 2,435.65)	1,664.56 (1,619.48, 1,709.64)	1,994.77 (1,943.16, 2,046.38)	2,700.81 (2,643.05, 2,758.57)

Continued

District	Pop.				Cases				Incidence/100,000*			
	2019	2020	2021	2022	2019	2020	2021	2022	2019	2020	2021	2022
Swat	2,346,589	2,395,868	2,446,181	2,49,7551	21,085	23,280	17,684	14,066	898.54 (873.53, 923.55)	971.67 (944.92, 998.42)	722.92 (692.53, 753.31)	563.19 (533.81, 592.57)
Dir Upper	874,219	892,578	911,322	930,460	12,883	11,434	12,011	7,234	1,473.66 (1,434.42, 1,512.90)	1,281.01 (1,243.91, 1,318.11)	1,317.98 (1,280.63, 1,355.33)	777.46 (740.58, 814.34)
Shangla	696,642	711,968	727,632	743,639	14,419	20,157	26,066	41,316	2,069.79 (2,023.69, 2,115.89)	2,831.17 (2,774.85, 2,887.49)	3,582.31 (3,515.63, 3,649.00)	5,555.92 (5,478.41, 5,633.43)
Chitral Upper	193,248	197,306	201,450	205,680	679	332	484	453	351.36 (323.58, 379.14)	168.27 (147.50, 189.04)	240.26 (216.15, 264.37)	220.25 (196.82, 243.68)
Mardan	2,383,250	2,435,682	2,489,267	2,544,031	45,446	48,968	57,322	82,013	1,906.89 (1,869.21, 1,944.57)	2,010.44 (1,971.21, 2,049.67)	2,302.77 (2,259.63, 2,345.91)	3,223.74 (3,171.82, 3,275.66)
Swabi	1,518,381	1,550,267	1,582,823	1,616,062	7,182	4,589	4,527	4,230	473.00 (456.88, 489.12)	296.01 (282.54, 309.48)	286.01 (272.90, 299.12)	261.75 (248.44, 275.06)
Charsadda	1,564,393	1,597,245	1,630,787	1,665,034	53,718	74,692	87,219	88,271	3,433.79 (3,389.57, 3,478.01)	4,676.30 (4,620.33, 4,732.27)	5,348.28 (5,287.39, 5,409.17)	5,301.45 (5,239.84, 5,363.06)
Nowshera	1,472,370	1,503,289	1,534,859	1,567,091	29,467	20,780	29,518	43,286	2,001.33 (1,958.33, 2,044.33)	1,382.30 (1,343.47, 1,421.13)	1,923.17 (1,880.45, 1,965.89)	2,762.19 (2,711.65, 2,812.73)
Peshawar	4,491,511	4,590,324	4,691,311	4,794,520	8,852	7,274	10,713	37,370	197.08 (183.52, 210.64)	158.46 (146.36, 170.56)	228.36 (213.77, 242.95)	779.43 (754.63, 804.23)

Note: Between 2019 and 2022, malaria incidence across districts showed substantial spatial and temporal variation. Southern districts, including Lakki Marwat, Tank, Bannu, Dera Ismail Khan, and Hangu, recorded the highest malaria incidence, consistently exceeding 2,000 cases per 100,000 population, with Lakki Marwat peaking at 9,600 cases per 100,000 population in 2022. By contrast, northern districts, including Abbottabad, Haripur, Mansehra, and Swat, exhibited markedly low incidence, often below 500 cases per 100,000 population, indicating low transmission potential or more effective control.

Abbreviation: Pop=population; *CI*=confidence interval.

* shown as incidence (95% *CI*).

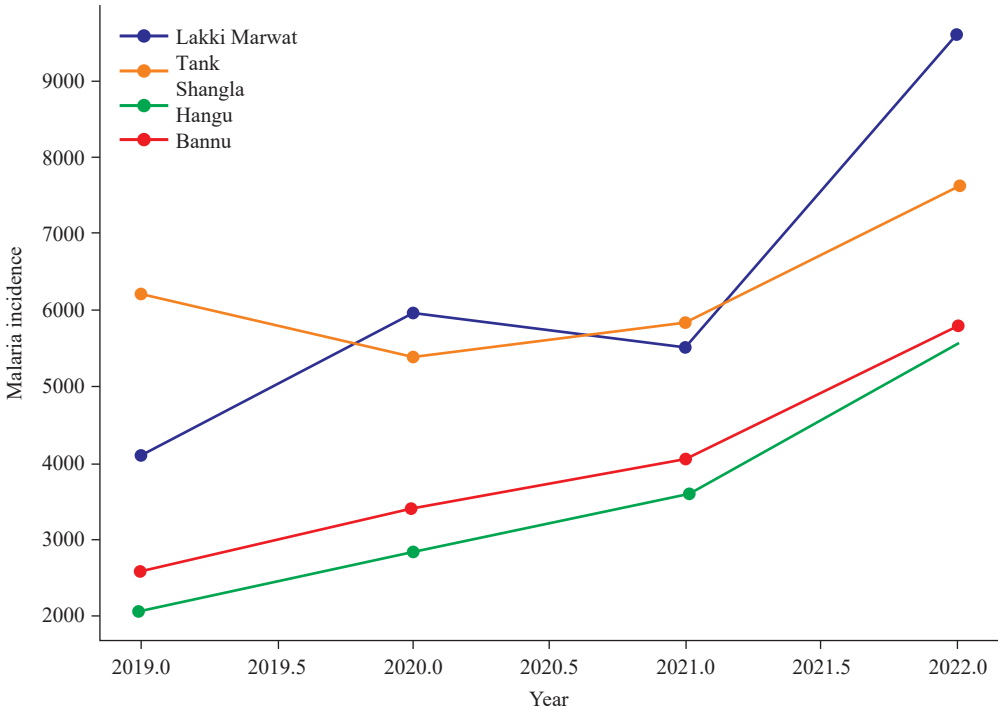

SUPPLEMENTARY FIGURE S1. Space–time clustering characterized by a progressive increase in malaria incidence from 2019 to 2022.
Note: ".0" in years means the start of the year.

Methods and Applications

Klebsiella pneumoniae Genome Database: A Global Resource for Genomic Surveillance of Dissemination, Pathogenicity, and Antimicrobial Resistance

Haijian Zhou[1]; Chongye Guo[2,3]; Guomei Fan[2,3]; Jinrui Hu[1]; Zhigang Cui[1]; Xiaoli Du[1]; Linhuan Wu[2,3,#]; Biao Kan[1,#]

ABSTRACT

Introduction: To address the escalating public health threat of hypervirulent and antibiotic-resistant *Klebsiella pneumoniae* (KP), we developed the Klebsiella pneumoniae Genome Database (KPGD; http://nmdc.cn/gcpathogen/kp) to strengthen global genomic surveillance of this pathogen.

Methods: KPGD integrates 75,987 genome assemblies from 122 countries with standardized annotations of serotypes, sequence types, antibiotic resistance genes (ARGs), virulence factors (VFs), and mobile genetic elements (MGEs). The platform offers interactive visualization modules and integrated analytical tools that enable real-time epidemiological monitoring and one-stop genomic analysis, thereby supporting global efforts to track the dissemination of resistant and hypervirulent KP (HvKp) and to inform infection control and antimicrobial stewardship strategies.

Results: Longitudinal analyses revealed that the emergence of HvKp is driven by the sustained expansion of carbapenem-resistant high-risk lineages under selection pressure from restricted, higher-tier antibiotics. Conjugative ARG-bearing plasmids carrying key resistance determinants largely mediate this expansion. In contrast, selection by first-line, narrower-spectrum antibiotics appears to favor the dissemination of virulence plasmids (predominantly IncFIB types) as a compensatory mechanism to offset resistance-associated fitness costs.

Conclusion: These findings collectively underscore the need for surveillance systems that simultaneously monitor high-risk lineages and the dissemination of ARGs and VFs — particularly via self-transmissible plasmids — to better understand and anticipate bacterial adaptation under diverse antibiotic pressures.

Klebsiella pneumoniae (KP) ranks among the leading causes of healthcare-associated infections worldwide, with high morbidity and mortality driven by carbapenem-resistant and hypervirulent strains The World Health Organization (WHO) listed KP as a critical pathogen on its Bacterial Priority Pathogens List in both 2017 and 2024 (*1*). Of particular concern are hypervirulent KP (hvKp) and carbapenem-resistant hvKp (CR-hvKp). High-risk clones such as NDM-positive ST147-KL64 (with mortality rates approaching 40%) (*2–3*) and ST23-KL1 (carrying rmpA/rmpA2, iroB, and/or iucA) are expanding rapidly — at an annual global growth rate of 59% and of 30% in China (*4*). These trends underscore the urgent need for systematic surveillance of carbapenem-resistant KP (CRKP), hvKp, and CR-hvKp.

Genomic surveillance provides high-resolution genetic insights that enable real-time reconstruction of transmission chains and prospective threat assessment. By elucidating pathogen evolution, dissemination patterns, and clinically relevant phenotypes, it strengthens public health responses (*5–6*). Clarifying the evolutionary trajectories of antimicrobial resistance (AMR) and virulence determinants further optimizes clinical decision-making and supports targeted infection control (*7*). This approach represents a paradigm shift from traditional phenotype-based monitoring, enabling outbreak tracing, epidemic forecasting, early warning of high-risk strains, and real-time assessment of emerging AMR and hypervirulence.

Discovering, surveying, and assessing the emergence and spread of hypervirulent KP clones and sequence types requires a comprehensive database of global KP genomes. Although public databases such as the National Center for Biotechnology Information (NCBI) are available, existing resources lack the integration of epidemiological metadata with standardized genomic annotations. To address these critical gaps in global KP surveillance, we established the Klebsiella pneumoniae Genome Database

(KPGD), which integrates sequence types, serotypes, antibiotic resistance genes (ARGs), virulence factors (VFs), mobile genetic elements (MGEs), and associated epidemiological metadata — including collection time and geographic origin. KPGD carries significant public health implications by enabling early warning of emerging high-risk clones, supporting outbreak investigations, and assisting public health agencies in monitoring the dissemination of hypervirulent and carbapenem-resistant KP.

METHODS

Data Source

KPGD integrates 75,987 KP genomes collected over more than 40 years from 122 countries. Of these, 71,132 publicly available genomes were retrieved from the National Center for Biotechnology Information (NCBI)(*8*), and 4,855 sequences were collected through national surveillance conducted by the Chinese Pathogen Identification Net (China PIN), which performs hospital-based sampling for febrile respiratory syndrome; KP isolates obtained from lower respiratory tract specimens testing positive by nucleic acid detection were cultured and sequenced. These 4,855 sequences originated from 170 cities across 29 provincial-level administrative divisions (PLADs) in China (Supplementary Figure S1, available at http://weekly.chinacdc.cn/), spanning a period of over 40 years. A major component of the database is the Chinese collection of 17,251 genomes, comprising 12,396 NCBI sequences combined with those from the China PIN. All 75,987 genome assemblies underwent uniform quality assessment using CheckM (Queensland University of Technology, Queensland, Australia, v1.2.2) (*9*). Genomes with completeness≥95%, contamination≤5%, and consistency≥95% were retained for downstream analysis.

Analysis Methods

Genomes in KPGD were curated and analyzed using the Global Catalogue of Pathogens (gcPathogen) frameworks and tools (*10–11*) (Figure 1 and Supplementary Material, available at http://weekly.chinacdc.cn/). Hyper-VFs (iroB, iucA, rmpA, and rmpA2) and resistance genes were manually curated on

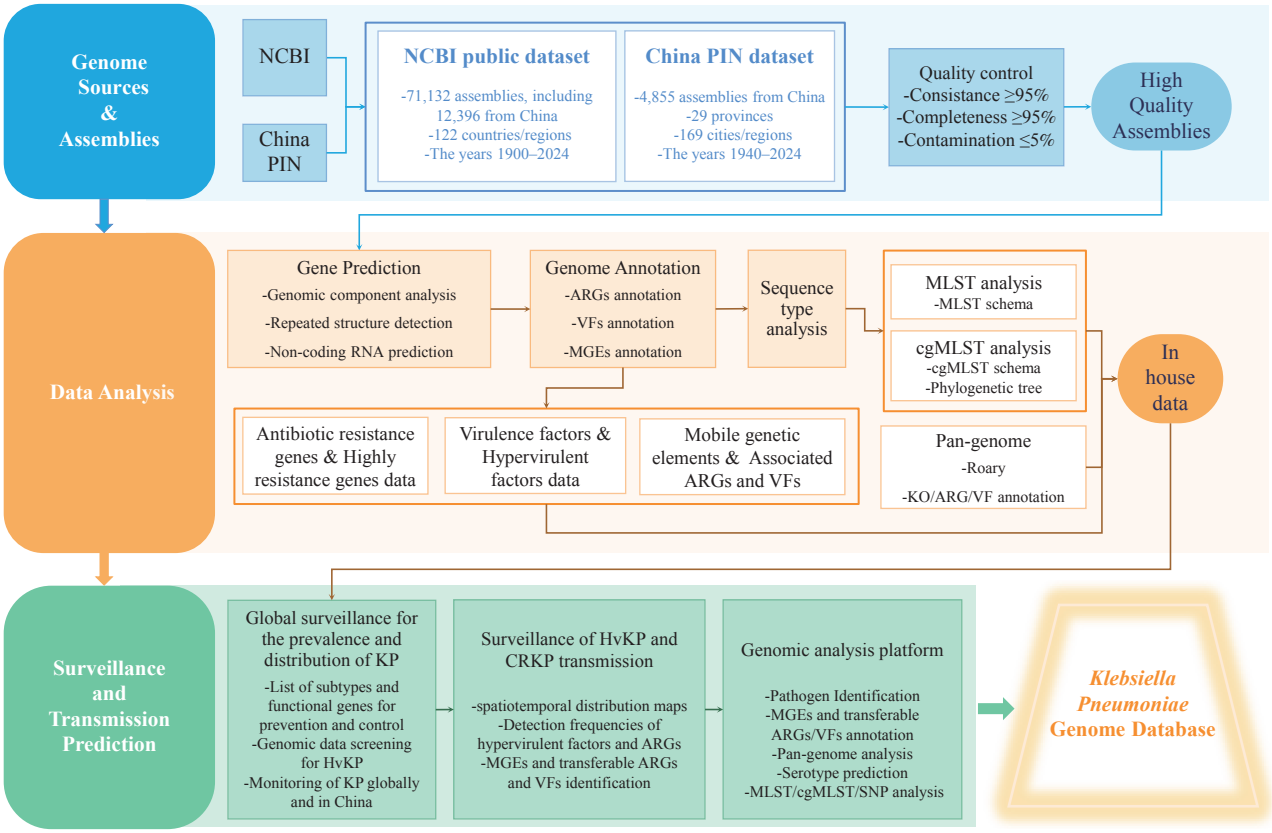

FIGURE 1. Data processing pipeline of the KPGD.
Abbreviation: KPGD=*Klebsiella pneumoniae* Genome Database; China PIN=Chinese Pathogen Identification Net.

the basis of a systematic literature review.

RESULTS

Overview of the KPGD Web Interface and Analytical Modules

The KPGD web platform (Figure 2A) provides comprehensive statistical summaries, including total genome counts and distributions of K/O antigens, hvKp strains, ARGs, sampling countries, and collection years. The "Genome Data" module supports advanced queries by WHO regions, serotypes, sequence types (STs), ARGs, and VFs. Search outputs appear in an interactive tabular format on a secondary page, integrating curated metadata with analytical results. The knowledge graph (Figure 2B) visualizes collaborative networks of research institutions and investigators, along with relevant publications and patents.

The AMR module identifies high-frequency, widely distributed ARGs across hosts and ecological niches. The MGE module maps mobile genetic elements harboring critical ARGs and hyper-VFs, enabling assessment of their horizontal transfer potential. The hvKp module captures the dynamics and epidemiological trends of hypervirulent strains (Figure 2C), while the pan-genome analysis module resolves core and accessory gene repertoires, including conserved resistance determinants across lineages.

By integrating these genetic insights with spatiotemporal, host, and clinical metadata, KPGD facilitates early detection of dissemination events, tracks the evolutionary trajectories of resistance and hypervirulence, and monitors the spread of high-risk MGEs — thereby providing a platform for proactive public health intervention. For example, the high-risk clones ST147_KL64_O2a, ST23_KL1_O1ab, and ST45_KL24_O2a were confined to a limited number of countries before 2010 but had spread globally by 2024, demonstrating clear international transmission. Specifically, ST147_KL64_O2a was detected in only 13 countries prior to 2010; its geographic range expanded to 40 countries by 2015 and further to 47 countries by 2024. Similarly, ST23_KL1_O1ab exhibited a pronounced dissemination pattern, with its country-level distribution increasing from 13 countries in 2010 to 32 countries by 2024. Meanwhile, ST45_KL24_O2a was initially confined to 6 countries before 2010, underwent rapid dissemination to reach 28 countries by 2015, and continued cross-border transmission, expanding further to 32 countries by 2024.

Additionally, KPGD offers five integrated one-stop online tools (Supplementary Material) for pathogen identification, Single Nucleotide Polymorphism (SNP) analysis, serotype prediction, detection of MGEs and transferable ARGs and VFs, and Core Gene Multilocus Sequence Typing (cgMLST) analysis (Figure 2D).

Temporal Dynamics and Evolutionary Trends of High-Risk KP Lineages

Genomic surveillance through KPGD reveals a dynamic and evolving risk landscape characterized by distinct evolutionary trajectories among high-risk KP lineages under different antibiotic selection pressures, as stratified by the World Health Organization (WHO) Access, Watch, Reserve (AWaRe) classification (*12*) (Figure 3A). These findings underscore the need for lineage-specific surveillance and intervention strategies.

Clonal group analyses identified several high-risk lineages (Figure 3A), notably ST11_KL64_O2a and ST258_KL107_O2afg, detected at elevated frequencies (peaking at around 0.2, particularly after 2016) under "Watch" antibiotic selection (carbapenems and other β-lactams). ST11_KL64_O2a persisted from 2010 to 2024 with pronounced enrichment among carbapenem-resistant isolates, indicating adaptation to last-resort therapies. ST307_KL102_O2afg peaked among carbapenem-resistant strains before 2015 (>0.07), potentially reflecting increased use of imipenem and meropenem during that period (*13*), before declining rapidly to below 0.1. ST147_KL64_O2a exhibited marked post-2020 expansion (around 0.04), especially among carbapenem- and ampicillin-resistant isolates. The hypervirulent lineage ST23_KL1_O1ab remained at low frequencies (0–0.05), although its recent increase among imipenem-resistant isolates suggests progressive acquisition of resistance to broad-spectrum β-lactams.

At the population level, resistance frequencies displayed distinct temporal patterns. Carbapenem-resistance ARGs increased steadily, with β-lactam ARGs among ertapenem- and meropenem-resistant isolates rising from near zero in 2010 to 0.15–0.3 by 2024. In contrast, cephalosporin resistance declined overall (below 0.25), while penicillin β-lactam resistance fluctuated between 0.1 and 0.7. These trends underscore a shifting AMR landscape and highlight lineage-specific evolutionary strategies under defined

FIGURE 2. Features of the KPGD Website. (A) KPGD homepage. (B) The Knowledge Graph page depicting global KP research networks; (C) The hvKp subpage summarizing datasets, spatiotemporal patterns, regional and country-level counts, and ARG/VF frequencies by ST, country, and habitat. (D) Phylogenetic clustering of high-risk KP ST23 clones using the KPGD cgMLST tool.

Note: For (B), it includes authors, institutions, publications, and patents. For (D), the 2019 isolate NMDC60197270 from China PIN clustered within the same phylogenetic branch as isolates from Bangladesh (2016 and 2017), India (2020), and Ghana (2021), suggesting potential transmission from these regions. Furthermore, the 2024 isolate NMDC60192954 clustered predominantly with isolates from Japan (2019–2020), indicating possible transmission from Japan.

Abbreviation: KPGD=*Klebsiella pneumoniae* Genome Database; China PIN=Chinese Pathogen Identification Net; ST=sequence type.

antibiotic pressures, illustrating the adaptive diversification of high-risk KP clones in response to therapeutic interventions.

Temporal dynamics of key carbapenem-resistance

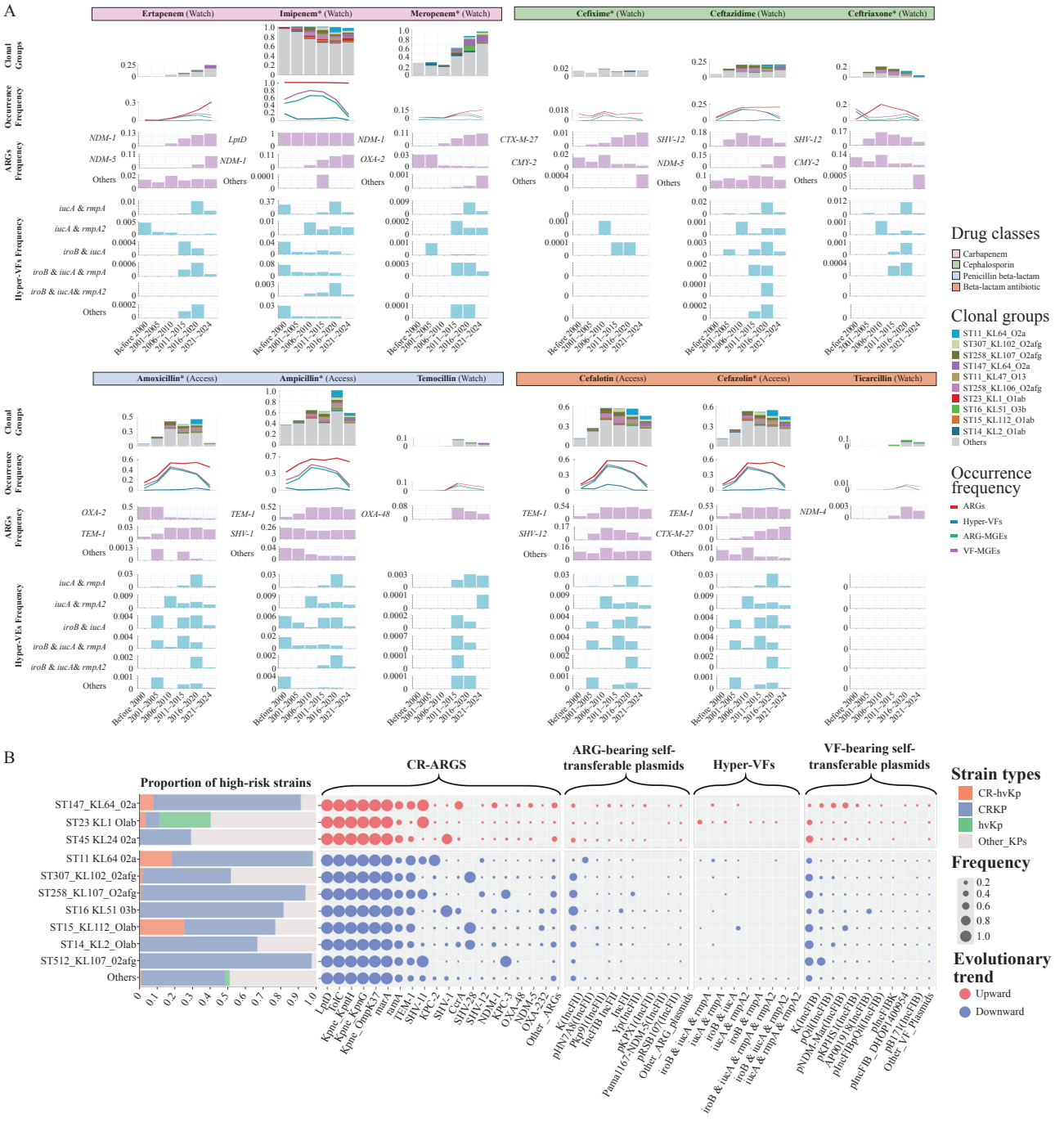

FIGURE 3. Risk Profiles and Evolutionary Trajectories of KP. (A) Longitudinal trends in ARGs, hyper-VFs, and major clonal lineages among KP isolates (before 2000–2024). (B) Risk assessment of the top 10 clonal lineages based on resistance and virulence determinants.

Note: For (A), Antibiotics are classified according to the WHO AWaRe framework ("Access" and "Watch"). Stacked bars represent the frequencies of the top 10 clonal lineages (with "Others" denoting remaining types). Line plots depict temporal changes in overall resistance and virulence frequencies under antibiotic pressure, while area charts summarize the occurrence of key ARGs and hyper-VFs. For (B), Bars represent different clonal groups, with colors indicating high-risk clones, including CR-hvKP, CRKP, and hvKP. Bubble plots illustrate the frequencies of carbapenem-resistance and hypervirulence genes, as well as the frequencies of self-transferable plasmids associated with these determinants. Red bubbles indicate an increasing trend for the corresponding clonal group, whereas blue bubbles indicate a decreasing trend.

Abbreviation: WHO=World Health Organization.

ARGs ("Watch" antibiotics) further emphasize this expansion (Figure 3A). NDM-1 emerged at 0.038 (2010–2015) and peaked at 0.13 (2022–2024). NDM-5 rose from undetectable levels to 0.11 by 2022–2024. In contrast, ARGs associated with "Access" antibiotics (e.g., TEM-1 in amoxicillin/ampicillin-resistant isolates) remained stable (around 0.1–0.5), consistent with their role in first-line therapy. Other ARGs (OXA-2, CMY-2, and CTX-M-27) persisted at low prevalence. Notably, the near-universal presence of LptD (frequency≈1.0) among imipenem-resistant isolates suggests a potential role in KP survival under carbapenem pressure. These ARGs were predominantly disseminated by conjugative IncFII-type plasmids, including K(IncFII), pHN7A8, and pKP91, whose frequencies fluctuated widely (0 to 0.6), underscoring their central role in the rapid horizontal transfer of carbapenem resistance.

Hyper-VF diversity was closely associated with resistance profiles across KP populations (Figure 3A). Among imipenem-resistant isolates ("Watch" antibiotic), hyper-VF richness was pronounced. Before 2000, the dominant combination (iroB, iucA, and rmpA) peaked at 0.08 and then declined steadily. Between 2011 and 2020, a two-factor combination (iucA and rmpA) predominated (around 0.04), surpassing all others. By 2024, all hyper-VF combinations had decreased to around 0.005. These hyper-VFs were largely disseminated by self-transmissible IncFIB-type virulence plasmids, including K(IncFIB) and pQil, peaking at around 0.5.

As shown in Figure 3B, ST23_KL1_O1ab harbored a substantially higher proportion of hvKP strains than other lineages. CR-hvKP strains were most frequently detected in ST15_KL2_O1ab, ST11_KL64_O2a, and ST147_KL64_O2a. Notably, the three clonal lineages displaying an increasing trend carried relatively low frequencies of ARG-bearing self-transferable plasmids. In contrast, all other clonal lineages (with decreasing trends) carried the ARG-bearing self-transferable plasmid K(IncFII), with the highest frequency exceeding 0.8. However, all lineages carried the VF-bearing self-transferable plasmid K(IncFIB), with a maximum frequency of approximately 0.6.

Time-series analyses revealed that fluctuations in virulence plasmid prevalence closely aligned with antibiotic selection regimes. Higher plasmid frequencies were associated with "Access" antibiotics, particularly first-generation cephalosporins (e.g., cefalotin and cefazolin). This suggests that virulence plasmid dissemination may be favored under first-line antibiotic pressure, potentially compensating for resistance-associated fitness costs and enhancing KP persistence.

CONCLUSIONS

This study establishes the Klebsiella pneumoniae Genome Database (KPGD) as a global resource for genomic surveillance, addressing the public health threats posed by the dissemination, pathogenicity, and antimicrobial resistance of hypervirulent and antibiotic-resistant lineages. By integrating 75,987 genomes from 122 countries with epidemiological metadata and standardized bioinformatic pipelines, KPGD enables high-resolution tracking of KP transmission, evolution, and risk patterns across decades and continents. These datasets can also be integrated into national monitoring systems, such as the China PIN, to support epidemic analysis, risk assessment, and early warning of high-risk KP clones.

Genomic surveillance revealed distinct evolutionary trajectories among high-risk lineages under differential antibiotic selection pressures. Clones including ST11_KL64_O2a and ST258_KL107_O2afg persisted under carbapenem-dominated "Watch" antibiotics, driven by horizontal acquisition of carbapenemase genes (e.g., NDM-1 and NDM-5) via conjugative IncFII-type plasmids. Temporal fluctuations in plasmid detection correlated with changes in antibiotic usage, underscoring their role as vectors for resistance dissemination.

The expansion of NDM-positive ST147_KL64_O2a represents a specific example of a high-risk clone in which carbapenem resistance and hypervirulence markers co-occur. This does not imply that NDM universally drives hypervirulence. Future studies should investigate region-specific associations between carbapenemase genes and hypervirulence markers.

Concurrently, a dynamic interplay between resistance and pathogenicity was observed. Under first-line "Access" antibiotic pressure, KP strains gained a selective advantage through acquisition of IncFIB-type virulence plasmids, facilitating the emergence of clones exhibiting both high pathogenicity and antimicrobial resistance (*14*).

Collectively, these findings provide a genomic framework for guiding public health strategies. KPGD serves as a foundational global resource for identifying emerging high-risk clones, elucidating the molecular drivers of their success, and tracking the horizontal

transfer of ARGs and VFs worldwide. Ensuring equitable access to such genomic platforms will be essential for coordinated international responses to the growing threat of hypervirulent and antimicrobial-resistant KP.

To this end, KPGD is an open and freely accessible web platform available at http://nmdc.cn/gcpathogen/kp. Unlike static genomic collections or one-time analytical studies, KPGD provides interactive real-time querying and integrated analytical modules for the global research community without registration or payment. Users worldwide can filter genomes by WHO region, serotype, ST, ARG, VF, collection time, and geographic origin.

Conflicts of interest: No conflicts of interest.

Funding: Supported by the National Key Research and Development Program of China (2023YFC2308800), the Self-Supporting Program of Guangzhou National Laboratory (SRPG22007), the Major Project of Guangzhou National Laboratory (GZNL2024A01025), and the Capital's Funds for Health Improvement and Research (CFH2024-1G-4361).

doi: 10.46234/ccdcw2026.092

[#] Corresponding authors: Linhuan Wu, wulh@ac.cn; Biao Kan, kanbiao@icdc.cn.

[1] National Key Laboratory of Intelligent Tracking and Forecasting for Infectious Diseases, National Institute for Communicable Disease Control and Prevention, Chinese Center for Disease Control and Prevention & Chinese Academy of Preventive Medicine, Beijing, China; [2] Chinese National Microbiology Data Center (NMDC), Beijing, China; [3] Beijing Research Center for Respiratory Infectious Diseases; Beijing Key Laboratory of Surveillance, Early Warning and Pathogen Research on Emerging Infectious Diseases, Beijing, China.

Submitted: April 18, 2026
Accepted: April 25, 2026
Issued: May 01, 2026

REFERENCES

1. WHO Bacterial Priority Pathogens List. Bacterial pathogens of public health importance to guide research, development and strategies to prevent and control antimicrobial resistance. Geneva: World Health Organization; 2024. Licence: CC BY-NC-SA 3.0 IGO. https://iris.who.int/server/api/core/bitstreams/1a41ef7e-dd24-4ce6-a9a6-1573562e7f37/content.
2. Di Pilato V, De Angelis LH, Aiezza N, Baccani I, Niccolai C, Parisio EM, et al. Resistome and virulome accretion in an NDM-1-producing ST147 sublineage of *Klebsiella pneumoniae* associated with an outbreak in Tuscany, Italy: a genotypic and phenotypic characterisation. Lancet Microbe 2022;3(3):e224 – 34. https://doi.org/10.1016/S2666-5247(21)00268-8.
3. Martin MJ, Corey BW, Sannio F, Hall LR, MacDonald U, Jones BT, et al. Anatomy of an extensively drug-resistant *Klebsiella pneumoniae* outbreak in Tuscany, Italy. Proc Natl Acad Sci USA 2021;118(48):e2110227118. https://doi.org/10.1073/pnas.2110227118.
4. Zhou HJ, Guo CY, Cui ZG, Hu JR, Du XL, Sun Y, et al. The epidemiology and hypervirulence of *Klebsiella pneumoniae* ST23 unveil epidemic risks in China and worldwide. Lancet Reg Health West Pac 2025;62:101661. https://doi.org/10.1016/j.lanwpc.2025.101661.
5. Lytras S, Lamb KD, Ito J, Grove J, Yuan K, Sato K, et al. Pathogen genomic surveillance and the AI revolution. J Virol 2025;99(2):e01601 – 24. https://doi.org/10.1128/jvi.01601-24.
6. David S, Reuter S, Harris SR, Glasner C, Feltwell T, Argimon S, et al. Epidemic of carbapenem-resistant *Klebsiella pneumoniae* in Europe is driven by nosocomial spread. Nat Microbiol 2019;4(11):1919 – 29. https://doi.org/10.1038/s41564-019-0492-8.
7. Loconsole D, Sallustio A, Sacco D, Santantonio M, Casulli D, Gatti D, et al. Genomic surveillance of carbapenem-resistant *Klebsiella pneumoniae* reveals a prolonged outbreak of extensively drug-resistant ST147 NDM-1 during the COVID-19 pandemic in the Apulia region (Southern Italy). J Glob Antimicrob Resist 2024;36:260 – 6. https://doi.org/10.1016/j.jgar.2024.01.015.
8. Kitts PA, Church DM, Thibaud-Nissen F, Choi J, Hem V, Sapojnikov V, et al. Assembly: a resource for assembled genomes at NCBI. Nucl Acids Res 2016;44(D1):D73 – 80. https://doi.org/10.1093/nar/gkv1226.
9. Parks DH, Imelfort M, Skennerton CT, Hugenholtz P, Tyson GW. CheckM: assessing the quality of microbial genomes recovered from isolates, single cells, and metagenomes. Genome Res 2015;25(7):1043 – 55. https://doi.org/10.1101/gr.186072.114.
10. Guo CY, Chen Q, Fan GM, Sun Y, Nie JY, Shen ZH, et al. gcPathogen: a comprehensive genomic resource of human pathogens for public health. Nucl Acids Res 2024;52(D1):D714 – 23. https://doi.org/10.1093/nar/gkad875.
11. Fan GM, Guo CY, Zhang Q, Liu DM, Sun QL, Cui ZG, et al. A secure visualization platform for pathogenic genome analysis with an accurate reference database. Biosafety Health 2024;6(4):235 – 43. https://doi.org/10.1016/j.bsheal.2024.07.003.
12. Sharland M, Zanichelli V, Ombajo LA, Bazira J, Cappello B, Chitatanga R, et al. The WHO essential medicines list AWaRe book: from a list to a quality improvement system. Clin Microbiol Infect 2022;28(12):1533 – 5. https://doi.org/10.1016/j.cmi.2022.08.009.
13. Wang LG, Chen H, Zhang YY, Tian Y, Hu XY, Wu J, et al. Global antibiotic consumption and regional antimicrobial resistance, 2010-21: an analysis of pharmaceutical sales and antimicrobial resistance surveillance data. Lancet Glob Health 2025;13(11):e1880 – 91. https://doi.org/10.1016/S2214-109X(25)00308-0.
14. Carvalho AG, Belém MGL, Rodrigues RS, Da Silva MEP, dos Santos Dorneles NW, Da Silva Lima NC, et al. Serotype distribution, virulence factors, and antimicrobial resistance profiles of *Streptococcus agalactiae* (Group B Streptococcus) isolated from pregnant women in the Brazilian Amazon. BMC Microbiol 2025;25(1):361. http://10.1186/s12866-025-04077-2.

SUPPLEMENTARY MATERIALS

Bioinformatic analysis of the genomes in the *Klebsiella pneumoniae* Genome Database (KPGD) was performed using the analysis tools within the gcPathogen one-stop analysis system (*1*), including pathogen identification, multilocus sequence typing (MLST), core genome multilocus sequence typing (cgMLST), pan-genome analysis, and genomic annotation for ARGs, VFs, and mobile genetic elements (MGEs) (Figure 1). A suite of one-stop online tools has been integrated into KPGD. The following section describes their primary workflows and the underlying software.

The Pathogen Identification Tool primarily employs bioinformatic software such as Kraken2 (*2*) and RNAmmer (*3*) for sequence similarity comparisons against reference libraries, generating optimal alignments for species identification. The results page displays the identified species, basic biological information, the corresponding reference genome, and detailed 16S rDNA data. The 16S rDNA BLAST search uses an e-value threshold of ≤1e-5, and the top 10 hits are retained based on bit-score. For ANI-based analysis, a consistency threshold of >95% is required for species assignment. If multiple species are detected, Kraken2 k-mer analysis is triggered; a species is considered confirmed if its k-mer abundance exceeds 80% and the second-ranked species abundance falls below 3%.

Genomic annotation is performed using the integrated annotation tool of the gcPathogen platform (*1*). It conducts genomic component analysis using PILER-CR v1.06 (*4*) for CRISPR array recognition, followed by repeat structure detection using TRF v4.07b (*5*). Non-coding RNA prediction is then carried out with tRNAscan-SE v1.4 (*6*) and RNAmmer v1.2. Finally, gene prediction is performed using Prodigal v2.6.3 (*7*). The predicted genes can be annotated against 11 commonly used functional databases, including KEGG (*8*), COG (*9*), NCBI-nr (*10*), CARD (*11*), CAZy (*12*), PHI (*13*), SwissProt (*14*), VFDB (*15*), Pfam (*16*), MetaCyc (*17*), and AntiSMASH (*18*). The alignment parameters are set as follows: query coverage >80%, subject coverage >80%, and sequence identity >90%.

The SNP Analysis Tool employs iVar (*19*) for SNP calling, Gubbins (*20*) to construct SNP matrices (excluding recombinant regions), and IQ-TREE 2 (*21*) for phylogenetic tree construction, with mutation site details displayed on the results page.

The Serotype Prediction Tool applies Kleborate (*22*), with the result file containing the species match degree, data quality, ST (sequence type), serotype, and other relevant details.

The MGE and Transferable ARGs and VFs Detection Tool leverages annotation software such as ISEScan (*23*) and MobileElementFinder (*24*) to annotate insertion sequences (IS), integrative conjugative elements (ICE), integrons (IN), plasmids, transposons (Tn), and their associated ARGs and VFs, presenting their types, names, genomic locations, and lengths. An ARG or VF is considered potentially transferable if it meets either of the following criteria: (i) the same IS element is present within 10 kb both upstream and downstream of the gene; or (ii) the gene is located within the sequence range of an ICE, integron, plasmid, phage, or transposon. These criteria are applied to assess horizontal transfer potential.

Built on chewBBACA (*25*), the cgMLST Analysis Tool enables schema creation and allele calling for both complete and draft genomes. With ≥3 genus- or species-level genomes uploaded, it generates visualized phylogenetic trees and result files. The cgMLST analysis tool enables phylogenetic clustering of closely related isolates. When these clusters are combined with spatiotemporal metadata (collection time and geographic origin), they can be used to infer potential transmission chains and support outbreak investigations.

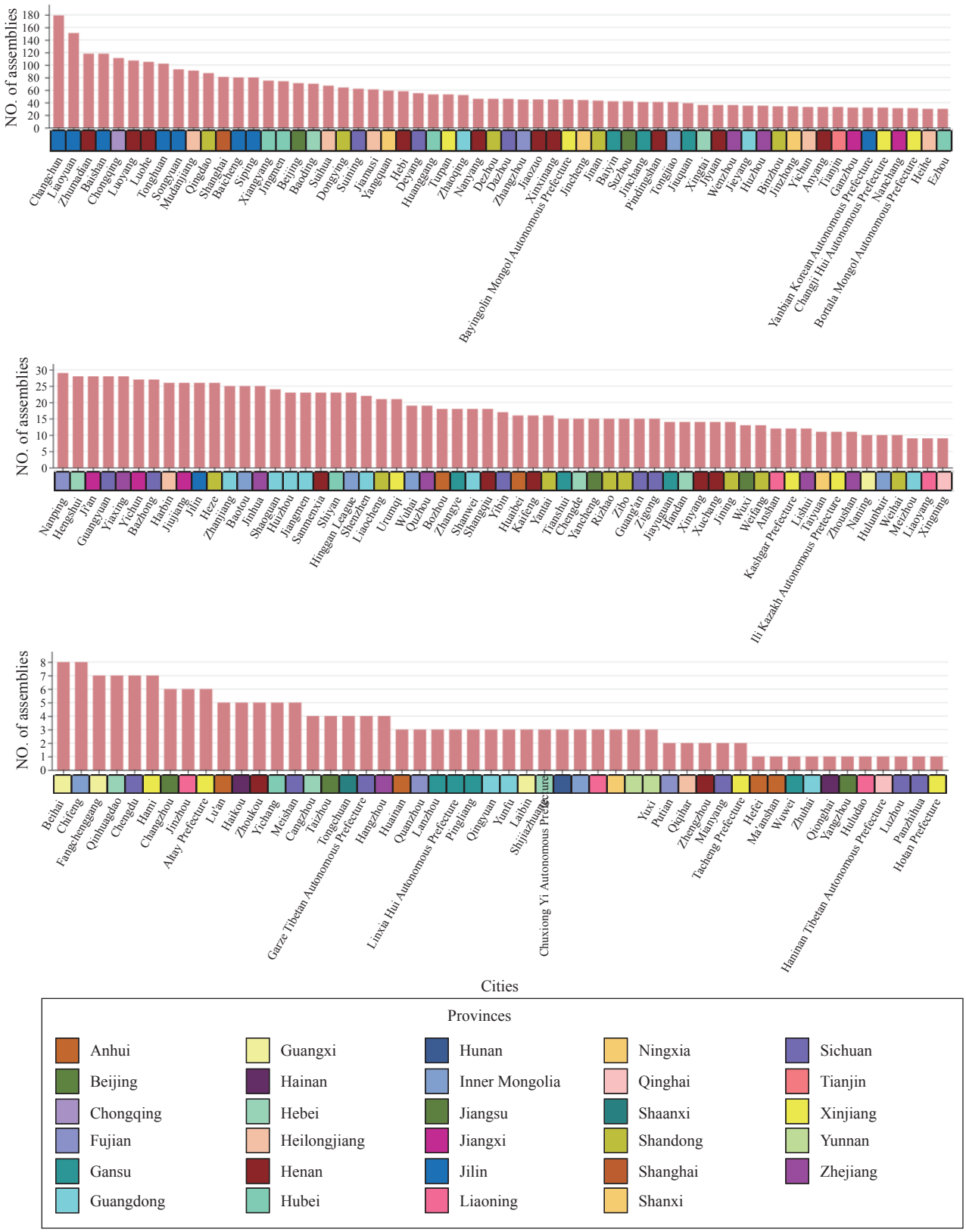

SUPPLEMENTARY FIGURE S1. Distribution of 4,855 China PIN-derived sequences across 29 PLADs and 169 cities in China.
Abbreviation: PLAD=provincial-level administrative division.

REFERENCES

1. Fan GM, Guo CY, Zhang Q, Liu DM, Sun QL, Cui ZG, et al. A secure visualization platform for pathogenic genome analysis with an accurate reference database. Biosafety Health 2024;6(4):235 – 43. https://doi.org/10.1016/j.bsheal.2024.07.003.
2. Wood DE, Lu J, Langmead B. Improved metagenomic analysis with Kraken 2. Genome Biol 2019;20(1):257. https://doi.org/10.1186/s13059-019-1891-0.
3. Lagesen K, Hallin P, Rødland EA, Stærfeldt HH, Rognes T, Ussery DW. RNAmmer: consistent and rapid annotation of ribosomal RNA genes. Nucl Acids Res 2007;35(9):3100 – 8. https://doi.org/10.1093/nar/gkm160.
4. Edgar RC. PILER-CR: fast and accurate identification of CRISPR repeats. BMC Bioinformatics 2007;8(1):18. https://doi.org/10.1186/1471-2105-8-18.
5. Gant TW, Sauer UG, Zhang SD, Chorley BN, Hackermüller J, Perdichizzi S, et al. A generic Transcriptomics Reporting Framework (TRF) for 'omics data processing and analysis. Regul Toxicol Pharmacol 2017;91(S1):S36 – 45. https://doi.org/10.1016/j.yrtph.2017.11.001.
6. Chan PP, Lin BY, Mak AJ, Lowe TM. tRNAscan-SE 2. 0: improved detection and functional classification of transfer RNA genes. Nucl Acids Res 2021;49(16):9077 – 96. https://doi.org/10.1093/nar/gkab688.
7. Hyatt D, Chen GL, LoCascio PF, Land ML, Larimer FW, Hauser LJ. Prodigal: prokaryotic gene recognition and translation initiation site identification. BMC Bioinformatics 2010;11(1):119. https://doi.org/10.1186/1471-2105-11-119.
8. Kanehisa M, Goto S. KEGG: Kyoto encyclopedia of genes and genomes. Nucl Acids Res 2000;28(1):27 – 30. https://doi.org/10.1093/nar/28.1.27.
9. Galperin MY, Wolf YI, Makarova KS, Vera Alvarez R, Landsman D, Koonin EV. COG database update: focus on microbial diversity, model organisms, and widespread pathogens. Nucl Acids Res 2021;49(D1):D274 – 81. https://doi.org/10.1093/nar/gkaa1018.
10. Sayers EW, Cavanaugh M, Clark K, Pruitt KD, Schoch CL, Sherry ST, et al. GenBank. Nucl Acids Res 2022;50(D1):D161 – 4. https://doi.org/10.1093/nar/gkab1135.
11. Alcock BP, Raphenya AR, Lau TTY, Tsang KK, Bouchard M, Edalatmand A, et al. CARD 2020: antibiotic resistome surveillance with the comprehensive antibiotic resistance database. Nucl Acids Res 2020;48(D1):D517 – 25. https://doi.org/10.1093/nar/gkz935.
12. Lombard V, Golaconda Ramulu H, Drula E, Coutinho PM, Henrissat B. The carbohydrate-active enzymes database (CAZy) in 2013. Nucl Acids Res 2014;42(D1):D490 – 5. https://doi.org/10.1093/nar/gkt1178.
13. Urban M, Cuzick A, Seager J, Wood V, Rutherford K, Venkatesh SY, et al. PHI-base: the pathogen-host interactions database. Nucl Acids Res 2020;48(D1):D613-20. http://dx.doi.org/10.1093/nar/gkz904.
14. McMillan LEM, Martin ACR. Automatically extracting functionally equivalent proteins from SwissProt. BMC Bioinformatics 2008;9(1):418. https://doi.org/10.1186/1471-2105-9-418.
15. Liu B, Zheng DD, Zhou SY, Chen LH, Yang J. VFDB 2022: a general classification scheme for bacterial virulence factors. Nucl Acids Res 2022;50(D1):D912 – 7. https://doi.org/10.1093/nar/gkab1107.
16. Mistry J, Chuguransky S, Williams L, Qureshi M, Salazar GA, Sonnhammer ELL, et al. Pfam: the protein families database in 2021. Nucl Acids Res 2021;49(D1):D412 – 9. https://doi.org/10.1093/nar/gkaa913.
17. Karp PD, Riley M, Paley SM, Pellegrini-Toole A. The MetaCyc database. Nucl Acids Res 2002;30(1):59 – 61. https://doi.org/10.1093/nar/30.1.59.
18. Blin K, Shaw S, Kloosterman AM, Charlop-Powers Z, Van Wezel GP, Medema MH, et al. antiSMASH 6. 0: improving cluster detection and comparison capabilities. Nucl Acids Res 2021;49(W1):W29 – 35. https://doi.org/10.1093/nar/gkab335.
19. Castellano S, Cestari F, Faglioni G, Tenedini E, Marino M, Artuso L, et al. iVar, an interpretation-oriented tool to manage the update and revision of variant annotation and classification. Genes 2021;12(3):384. https://doi.org/10.3390/genes12030384.
20. Croucher NJ, Page AJ, Connor TR, Delaney AJ, Keane JA, Bentley SD, et al. Rapid phylogenetic analysis of large samples of recombinant bacterial whole genome sequences using Gubbins. Nucl Acids Res 2015;43(3):e15. https://doi.org/10.1093/nar/gku1196.
21. Minh BQ, Schmidt HA, Chernomor O, Schrempf D, Woodhams MD, Von Haeseler A, et al. IQ-TREE 2: new models and efficient methods for phylogenetic inference in the genomic era. Mol Biol Evol 2020;37(5):1530 – 4. https://doi.org/10.1093/molbev/msaa015.
22. Lam MMC, Wick RR, Watts SC, Cerdeira LT, Wyres KL, Holt KE. A genomic surveillance framework and genotyping tool for *Klebsiella pneumoniae* and its related species complex. Nat Commun 2021;12(1):4188. https://doi.org/10.1038/s41467-021-24448-3.
23. Xie ZQ, Tang HX. ISEScan: automated identification of insertion sequence elements in prokaryotic genomes. Bioinformatics 2017;33(21):3340 – 7. https://doi.org/10.1093/bioinformatics/btx433.
24. Johansson MHK, Bortolaia V, Tansirichaiya S, Aarestrup FM, Roberts AP, Petersen TN. Detection of mobile genetic elements associated with antibiotic resistance in *Salmonella enterica* using a newly developed web tool: MobileElementFinder. J Antimicrob Chemother 2021;76(1):101 – 9. https://doi.org/10.1093/jac/dkaa390.
25. Silva M, Machado MP, Silva DN, Rossi M, Moran-Gilad J, Santos S, et al. chewBBACA: a complete suite for gene-by-gene schema creation and strain identification. Microb Genom 2018;4(3):e000166. https://doi.org/10.1099/mgen.0.000166.

Youth Editorial Board

Indexed by Science Citation Index Expanded (SCIE), Social Sciences Citation Index (SSCI), PubMed Central (PMC), Scopus, Chinese Scientific and Technical Papers and Citations, and Chinese Science Citation Database (CSCD)

The inauguration of *China CDC Weekly* is in part supported by Project for Enhancing International Impact of China STM Journals Category D (PIIJ2-D-04-(2018)) of China Association for Science and Technology (CAST).

CHINA CDC WEEKLY

CCDC weekly

Vol. 8 No. 18 May 1, 2026

中国疾病预防控制中心周报(英文)

Responsible Authority
National Disease Control and Prevention Administration

Sponsor
Chinese Center for Disease Control and Prevention &
Chinese Academy of Preventive Medicine

Editor-in-Chief
Jianwei Wang

Editing and Publishing
China CDC Weekly Editorial Office
No.155 Changbai Road, Changping District, Beijing, China
Tel: 86-10-63150501, 63150701
Email: weekly@chinacdc.cn

Printing: Beijing Kexin Printing Co., Ltd

Complimentary Access

CSSN
ISSN 2096-7071 (Print)
ISSN 2097-3101 (Online)
CN 10-1629/R1